iScience

CellPress
OPEN ACCESS

Article

Interleukin-2 receptor signaling acts as a checkpoint that influences the distribution of regulatory T cell subsets

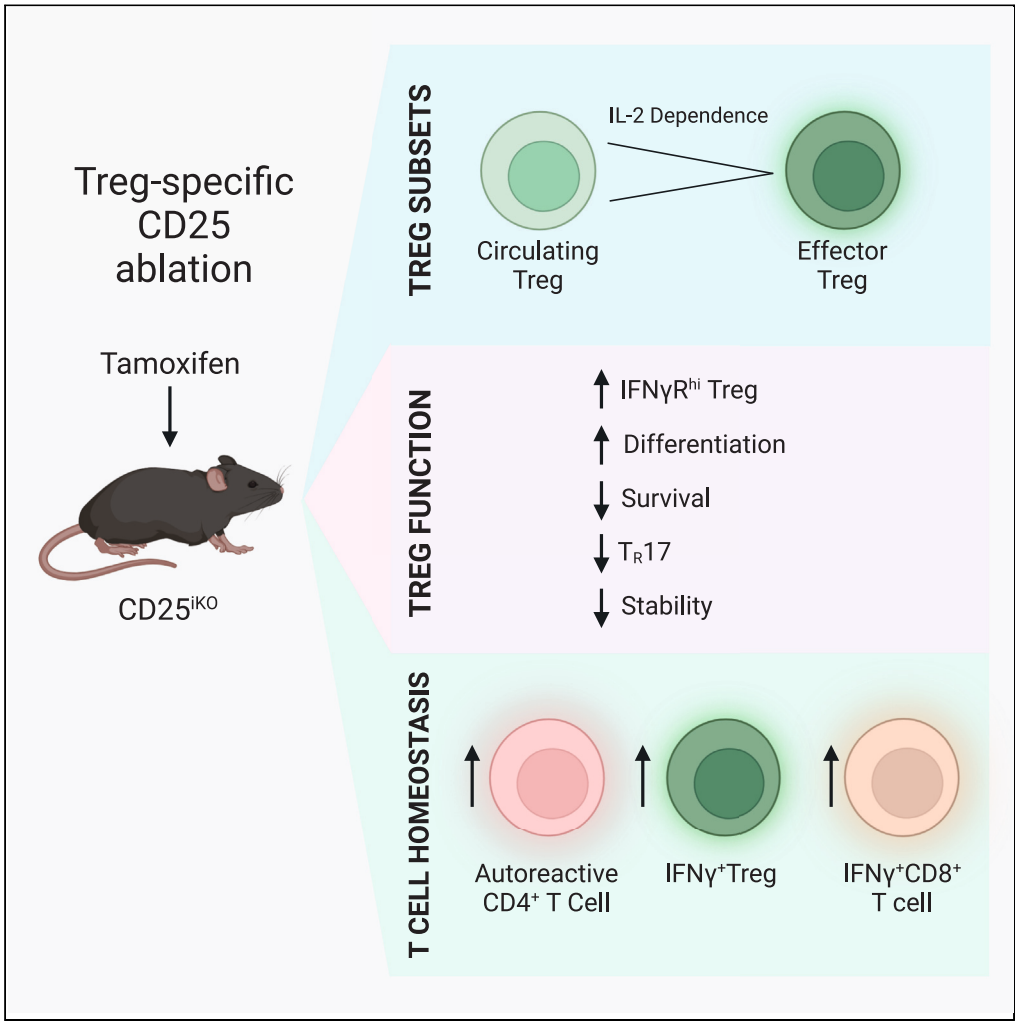

Acacia N. Shouse, Alejandro V. Villarino, Thomas R. Malek

tmalek@med.miami.edu

Highlights

IL-2 supports the survival of cTreg and eTregs, but cTregs are more dependent on IL-2

IL-2 programs several molecular signals for eTregs at the cTreg stage

Homeostatic levels of IL-2 restrain the development of eTregs from cTreg precursors

IL-2 uniquely influences the development IFNγR1^{+} eTregs, T_{FR} and T_R17 cells

Shouse et al., iScience 27, 111248
December 20, 2024
https://doi.org/10.1016/j.isci.2024.111248

iScience

CellPress
OPEN ACCESS

Article

Interleukin-2 receptor signaling acts as a checkpoint that influences the distribution of regulatory T cell subsets

Acacia N. Shouse,[1] Alejandro V. Villarino,[1] and Thomas R. Malek[1,2,*]

SUMMARY

Regulatory T cells (Tregs) require IL-2 for survival in the periphery, yet how IL-2 shapes Treg heterogeneity remains poorly defined. Here we show that inhibition of IL-2R signaling in post-thymic Tregs leads to a preferential early loss of circulating Tregs (cTregs). Gene expression of cTregs was more dependent on IL-2R signaling than effector Tregs (eTregs). Unexpectedly, ablation of IL-2R signaling in cTregs resulted in increased proliferation, expression of eTreg genes, and enhanced capacity to develop into eTregs. Thus, IL-2R signaling normally acts as a checkpoint to maintain cTreg homeostasis while restraining their development into eTregs. Loss of IL-2R signaling also alters the distribution of eTreg subsets, with increased IFNγR1$^+$ eTregs and CXCR5$^+$ PD-1$^+$ T follicular regulatory (T_{FR}) cells but decreased intestinal RORγt$^+$ T_R17 cells. These changes lower eTreg suppressive function supporting expansion of IFNγ-secreting T effector cells. Thus, IL-2R signaling also safeguards Treg function and licenses differentiation of specialized eTregs.

INTRODUCTION

Regulatory T cells (Tregs) are essential for maintaining peripheral self-tolerance. Relatively high and constitutive expression of the high-affinity interleukin-2 receptor (IL-2R) allows Tregs preferential access to interleukin-2 (IL-2). Indeed, multiple studies have demonstrated that IL-2 is essential for Treg development, homeostasis and function.[1–4] IL-2 released by T cells undergoing thymic selection allows for generation and functional maturation of Foxp3$^+$ Tregs prior to their entrance into the periphery.[5–8] Until recently, IL-2's essential role in thymic development has obscured its study in post-thymic Tregs. However, inducible deletion of CD25 selectively in Tregs has permitted the study of IL-2R signaling in post-thymic mouse Tregs. Previous work with this model has shown that Tregs continue to require IL-2 for their survival after exiting the thymus,[1] largely secreted by autoreactive T cells.[9] Fate mapping studies of CD25-deficient peripheral Tregs revealed that they fail to persist if they do not encounter IL-2.[1,10] This loss of Tregs takes time to unfold (12–16 weeks). Moreover, CD25-deficient peripheral Tregs are characterized by increased apoptosis and oxidative stress while exhibiting signs of mitochondrial dysfunction and reduced transcription of key enzymes for lipid and cholesterol biosynthetic pathways. The glycolytic activity and functional activity of peripheral Tregs were also reduced, but Treg stability was maintained.[1,10]

Tregs are a heterogeneous population of cells unified by expression of the transcription factor Foxp3. They are broadly categorized as circulating Tregs (cTregs) or effector Tregs (eTregs).[11,12] In normal mice, CD62L^{hi} CCR7$^+$ cTregs are typically long-lived resting Tregs that readily circulate through the spleen and lymph nodes, but at a much lesser extent through non-lymphoid tissues.[13,14] This subset has the highest expression of the high-affinity IL-2R and plays an essential role in controlling autoreactive CD4$^+$ T cells in secondary lymphoid tissues in part by binding and sequestering available IL-2.[9] cTregs are also precursors that give rise to eTregs, which differentiate in response to T cell receptor (TCR) signaling and/or inflammation.[15,16] Conversely, eTregs express lower amounts of the high affinity IL-2R but more 'effector' molecules, e.g., ICOS, CD69, CTLA-4, and IL-10[11]. eTregs show greater heterogeneity than cTregs, that express chemokines receptors that promote migration into non-lymphoid tissues where many persist and respond to a wide variety factors influencing their transcriptional regulation.[14,17,18] eTregs co-opt transcription factors associated with conventional effector T cells (Teff), thus tailoring them to suppress Teff subsets. For example, Tbet$^+$ Tregs (T_R1) and IRF4$^+$ Tregs (T_R2) are linked to suppression of T_H1 and T_H2 responses, respectively.[19,20] Bcl-6$^+$ CXCR5$^+$ PD-1$^+$ T follicular regulatory (T_{FR}) cells play a critical role in controlling the germinal center response[21–23] and RORγt$^+$ CCR6$^+$ ICOS$^+$ (T_R17) Tregs are important for regulating T_H17 inflammation in the intestine and other sites.[24–28]

A prevailing concept is that IL-2 plays a more important role for cTregs than eTregs.[1,13] Consistent with this notion, T_{FR} cells differentiate in environments with low IL-2, which allows for the upregulation of their subset-specific transcription factor Bcl-6.[29] However, fate mapping studies indicate not only cTregs, but also eTregs, cannot survive without IL-2R signaling, implicating it in both Tregs subsets.[1,10] Moreover,

[1]Department of Microbiology and Immunology, Miller School of Medicine, University of Miami, Miami, FL 33136, USA
[2]Lead contact
*Correspondence: tmalek@med.miami.edu
https://doi.org/10.1016/j.isci.2024.111248

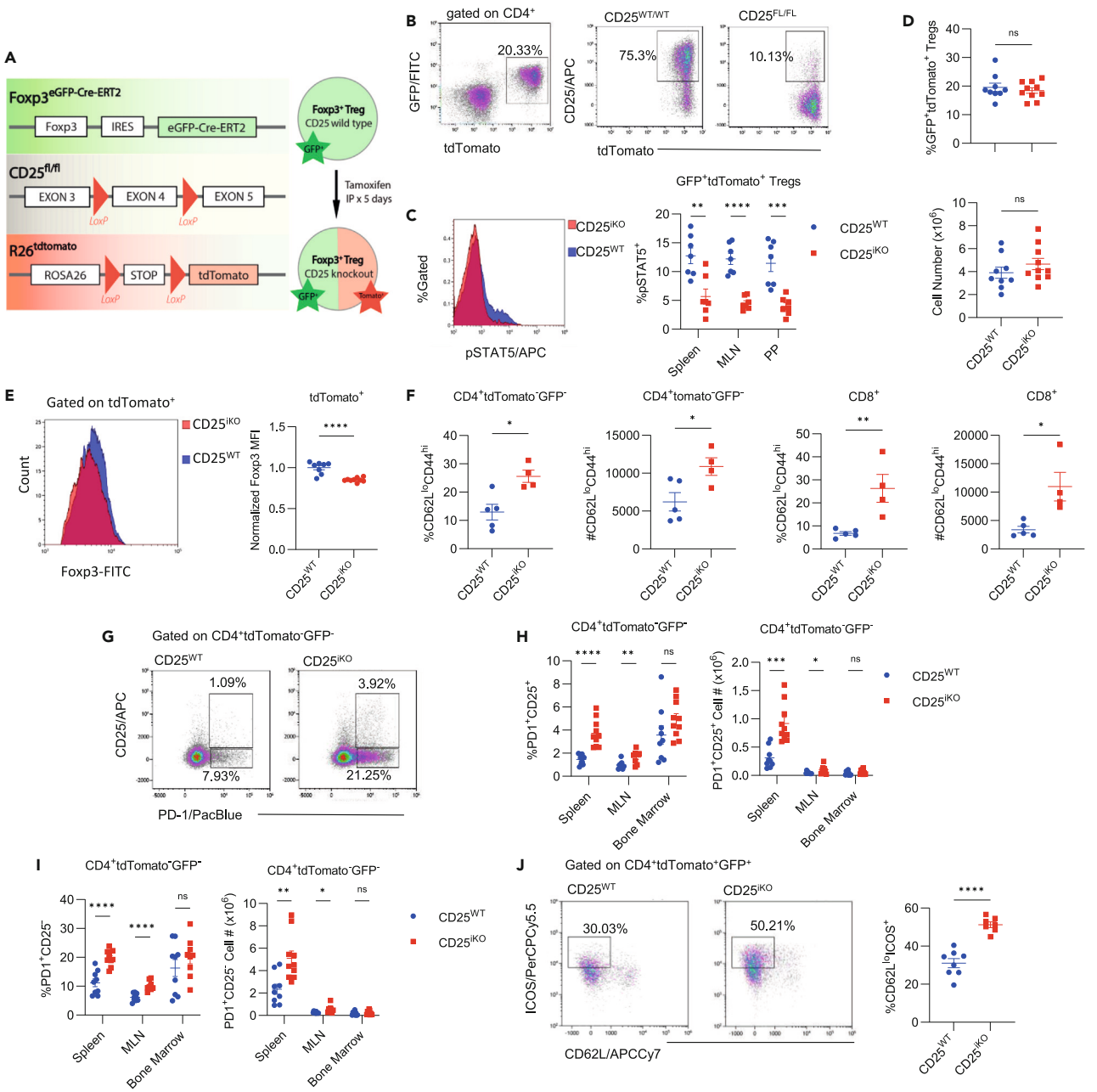

Figure 1. Inducible Treg-deletion of CD25 leads to activation of autoreactive T cells

(A) Schematic of the CD25^{iKO} mouse model incorporating three constructs, Foxp3$^{eGFP-Cre-ERT2}$, CD25$^{FL/FL}$ and R26^{tdTomato}. CD25 is knocked out upon the administration of tamoxifen. Mice lacking the CD25$^{FL/FL}$ construct are used as CD25^{WT} controls.

(B) Identification of GFP^{+} tdTomato^{+} Tregs by flow cytometry and assessment of CD25 expression by GFP^{+} tdTomato^{+} splenic Tregs from CD25^{WT} vs. CD25^{iKO} mice.

(C) Ex vivo pSTAT5 staining by Tregs from spleen, mesenteric lymph nodes (MLN) and Peyer's Patches (PP) of CD25^{WT} and CD25^{iKO} mice. Cells are gated on GFP^{+} tdTomato^{+} Tregs with representative flow cytometry histograms (left) and quantitative data (right).

(D) Frequencies and numbers of GFP^{+} tdTomato^{+} Tregs in the spleen.

(E) Foxp3 MFI from CD25^{WT} or CD25^{iKO} splenocytes after fixation and staining with anti-Foxp3.

(F) At 12 days post-tamoxifen, frequency and numbers of activated CD62L^{lo}CD44^{hi} CD4^{+} tdTomato^{-} GFP^{-} conventional T cells (left) and CD8^{+} T cells (right) in the blood from CD25^{WT} and CD25^{iKO} mice.

(G) Representative flow cytometry dot plots to measure CD4^{+} PD-1^{+} CD25^{+} and CD4^{+} PD-1^{+} CD25^{neg} autoreactive T cells in the spleen.

(H) Proportion and number of CD4^{+} PD-1^{+} CD25^{+} autoreactive T cells.

(I) Proportion and number of CD4^{+} PD-1^{+} CD25^{neg} autoreactive T cells.

Figure 1. *Continued*

(J) Representative flow cytometry dot plots (left) and quantitative data (right) for expression of CD62L and ICOS by $CD4^+$ Tregs in $CD25^{WT}$ and $CD25^{iKO}$ mice. All data were collected at 10 days post-tamoxifen treatment unless otherwise stated. Data (n = 4–5, E; n = 8–10, C, D, G-I) from at least two replicate experiments were analyzed by an unpaired t test. *p < 0.05, **p < 0.01, ***p < 0.001, ****p < 0.0001.

development of $Klrg1^+$ terminally differentiated eTregs in the gut mucosa depends on IL-2R signaling.[30] Here, we use tamoxifen-inducible Treg-specific knockout of CD25 to directly study the role of IL-2R signaling across post-thymic Treg subsets. Our findings indicate that IL-2R signaling impacts both cTregs and eTregs, acting as a checkpoint to restrain cTreg to eTreg differentiation while also influencing the development of specialized eTregs, particularly $IFN\gamma R1^+$ eTregs, T_{FR} and T_R17.

RESULTS

Inducible Treg-deletion of CD25 leads to activation of autoreactive T cells

To investigate the contribution of IL-2R signaling on post-thymic Treg subsets, CD25 was selectively and inducibly deleted on peripheral Tregs (Figure 1A). Mice bearing $Foxp3^{GFP\text{-}cre\text{-}ERT2}$ contain a GFP reporter linked to a tamoxifen-inducible cre recombinase expressed from the Foxp3 locus.[31] When these mice were bred to mice with a floxed-stop tdTomato reporter ($Rosa26^{tdTomato}$),[32] tamoxifen administration allows for constitutive expression and heritable cell labeling by tdTomato in a Foxp3-dependent fashion. Further breeding with mice bearing $CD25^{FL/FL}$ causes CD25 expression to be knocked out upon tamoxifen administration ($CD25^{iKO}$), thus allowing for ablation of post-thymic IL-2R signaling in Tregs. Control mice ($CD25^{WT}$) were tamoxifen-treated CD25 wild-type (WT) mice bearing $Foxp3^{GFP\text{-}cre\text{-}ERT2}$ and $Rosa26^{tdTomato}$.

Ten days post-tamoxifen, approximately 80%–90% of GFP^+ $tdTomato^+$ Tregs were $CD25^{neg}$ (Figure 1B) and pSTAT5 expression was reduced 2- to 3-fold when measured directly *ex vivo* (Figure 1C). Because a small proportion of GFP^+ $tdTomato^+$ Tregs retain CD25, $CD25^{iKO}$ Tregs were gated as $CD25^{neg}$ for all subsequent analyses. Importantly, the proportion and number of Tregs in the spleen at this timepoint were unchanged, indicating that the IL-2-dependent survival defect was not yet evident (Figure 1D), however there was a small decrease in Foxp3 expression (Figure 1E). Thus, analyses of the targeted cells were usually conducted on day 10–12 post-tamoxifen based on high efficiency of tdTomato expression (Figure 1B) and the kinetics of CD25 knockout (Figure S1A).

At 12 day post-tamoxifen, activated $CD62L^{lo}$ $CD44^{hi}$ $CD4^+$ and $CD8^+$ T cells increased in the spleen of $CD25^{iKO}$ mice (Figure 1F). Past work indicates that this represents an early autoimmune-related characteristic of mice whose Tregs have impaired IL-2R signaling.[31] $CD25^+$ $PD\text{-}1^+$ and $CD25^-$ $PD1^+$ $CD4^+$ autoreactive T cells were also increased in the spleen and lymph nodes (Figures 1G–1I).[9] These data suggest that rapid and efficient reduction of CD25 on Tregs has lowered their suppressive activity, consistent with previous reports.[2,10] T cell activation may result from impaired capture of IL-2 by Tregs, making IL-2 more available for activated T cells. Indeed, this is one mechanism by which Tregs suppress autoreactive T cells.[9] However, $CD25^{iKO}$ mice appeared outwardly normal through all observed time periods (8–9 months), and their autoimmunity did not progress. Autoimmunity is likely limited in $CD25^{iKO}$ mice due to expression of CD25 by new thymic emigrants, based on Tregs found on day 42 post-tamoxifen that expressed GFP but not tdTomato (Figure S1B) and by peripheral Tregs that escaped tamoxifen-dependent CD25 deletion (Figure 1B).

The cTreg transcriptome is more dependent on IL-2R signaling than that of eTregs

Previous work has shown that genes associated with eTregs are enriched when total Tregs were analyzed from $CD25^{iKO}$ mice.[1] Accordingly, we found that spleens of $CD25^{iKO}$ mice had a higher abundance of $CD62L^{lo}$ $ICOS^{hi}$ eTregs (Figure 1J), despite their reduced suppressive function. To identify CD25-dependent transcriptional programs that may underlie this change in Treg subset distribution, bulk RNA-seq was performed on cTreg and eTreg subsets from $CD25^{WT}$ and $CD25^{iKO}$ mice. $tdTomato^+$ GFP^+ $CD62L^{hi}$ cTregs and $tdTomato^+$ GFP^+ $CD62L^{lo}$ eTregs were purified from pooled spleens and lymph nodes of $CD25^{WT}$ and $CD25^{iKO}$ mice, and the latter were further sorted to remove any $CD25^+$ cells (Figure S2A). 1349 and 279 differentially expressed genes (DEGs) were identified between $CD25^{WT}$ and $CD25^{iKO}$ cTregs and eTregs, respectively (Figure 2A). These include genes that are up and down-regulated upon ablation of CD25. Notably, most DEGs from eTregs (221 of 279 DEGs; 79.2%) overlap with cTregs. Thus, the cTreg transcriptome is more dependent on CD25 expression and IL-2R signaling than eTregs.

K-means clustering of all DEGs showed that those in heatmap clusters 1–2, and 6–8 were coordinately increased or decreased in cTregs and eTregs after $CD25^{iKO}$ (Figure 2B). This preserved directionality is consistent with co-regulation of CD25-dependent gene expression between subsets, but the magnitude of these changes often differed by subset. Consistent with their greater reliance on CD25, DEGs in clusters 3–5, and 9 were only detected in cTregs after $CD25^{iKO}$. Yet, the genes in clusters 5 and 9 were also highly expressed in eTregs, suggesting that the cTreg transcriptome becomes more like that of eTregs after loss of IL-2R signaling. Indeed, $CD25^{iKO}$ cTregs express higher levels of many suppressive mediators typical of eTregs (Figure S2B).

As expected, the IL-2/STAT5 pathway was significantly enriched in both $CD25^{WT}$ cTregs and eTregs and $CD25^{iKO}$ cTregs by hypergeometric testing (Figure S2C). Most of the genes within this pathway that had the greatest fold changes were the same in each subset, but the magnitude of those changes was often greater in cTregs (Figure 2C). However, *Eomes* was uniquely enriched in $CD25^{iKO}$ cTregs, suggesting that it may underpin cTreg-specific effects of IL-2R signaling. Indeed, Eomes is responsible for the upregulation of effector genes in T cells and may induce effector genes in cTregs in the setting of low IL-2R signaling.[33]

GSEA revealed that many pathways were similarly affected across subsets, including MYC Targets, Interferon Gamma Response, Interferon Alpha Response and Complement (Figure 2D). IL-2R signaling may normally restrain the response to IFNγ in Tregs since the Interferon

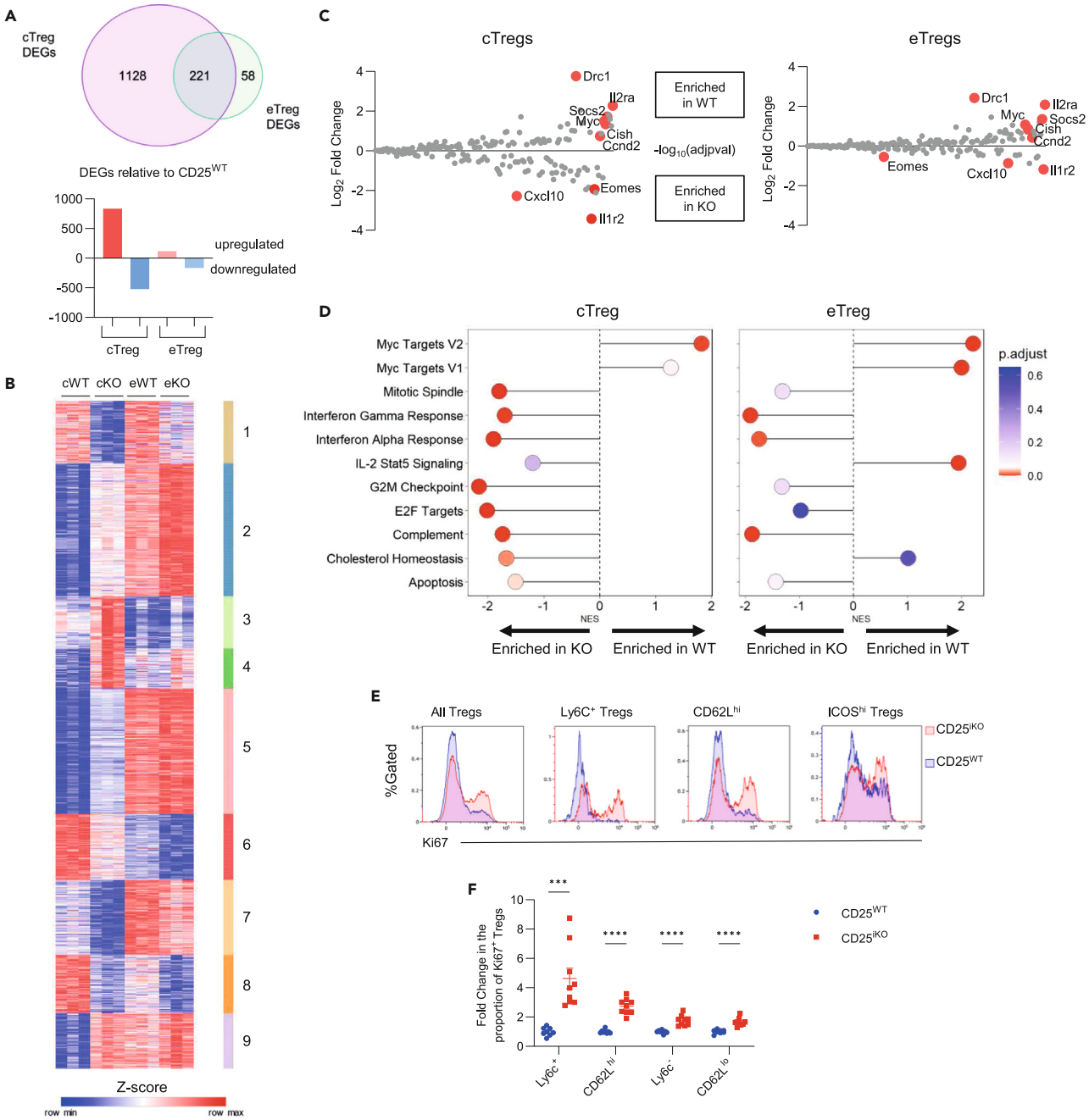

Figure 2. The cTreg transcriptome is more dependent on IL-2 signaling than that of eTregs

(A) Spleens and lymph nodes were pooled from 2 to 3 mice per replicate (n = 3/group), FACS-purified for CD62L^{hi} and CD62L^{lo} Treg subsets and subjected to bulk RNA-seq. The number of differentially expressed genes (DEGs) were determined (>1.5-fold with adjusted p-val <0.05).

(B) Heatmap of the DEGs displayed in A. The heatmap (broadinstitute.com/morpheus) was generated using TPMs converted to Z score and clustered by K-means.

(C) Genes from the Hallmark IL/2-STAT5 pathway were plotted as Log_2FC vs. log_{10}(adjpval). The genes that were the most differentially expressed in cTregs are highlighted by red dots in both plots.

(D) GSEA was performed and the top Hallmark pathways for each Treg subset were plotted for their enrichment score (x axis) and adjusted p value (color).

(E) Representative flow cytometry histograms of Ki67 expression by various Tregs subsets based on the indicated markers for CD25^{WT} and CD25^{iKO} Tregs.

(F) Quantitative data from (E).Data (n = 8, F) from two replicate experiments were analyzed by unpaired t test. ***p < 0.001, ****p < 0.0001.

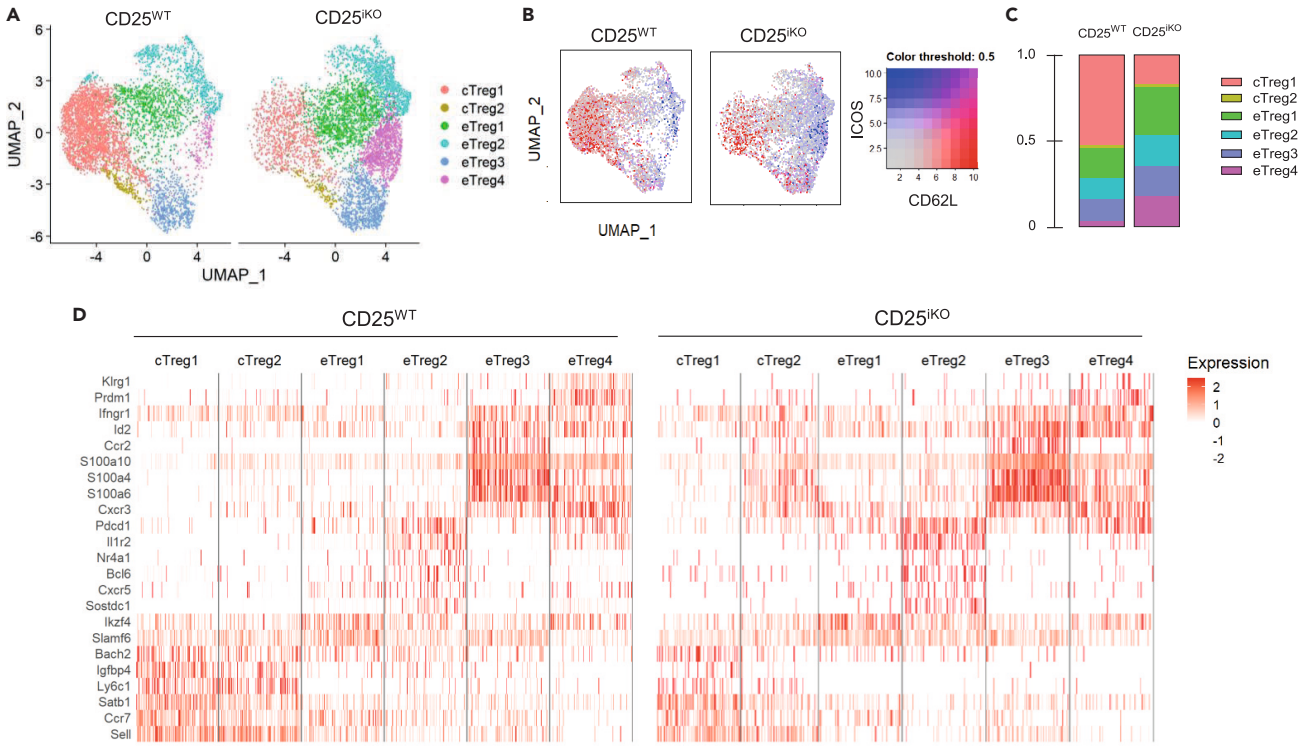

Figure 3. IL-2R signaling influences the proportion of cTreg and eTreg subsets

(A) scRNA-seq of FACS purified CD25^{iKO} and CD25^{WT} Tregs, each pooled from 2 spleens. The resulting data were merged and UMAP distribution of Treg clusters are then shown for the indicated Tregs.

(B) CD62L (red) and Icos (blue) expression overlayed onto the UMAP from Figure 4A for the indicated Tregs.

(C) Relative proportional changes of 5 clusters of Tregs (Figure 4A) from the indicated Tregs.

(D) Heatmaps of transcript expression between CD25^{iKO} and CD25^{WT} Tregs for cluster defining genes with relative expression level shown by the color bar on the right. Cluster-defining genes (Log_2FC >0.25, adjusted p-value <0.05) were determined using MAST by comparing the transcripts within each cluster compared to all other clusters.

Gamma Response pathway was significantly upregulated in both subsets. *Myc* is a well-recognized target of IL-2 signaling[34,35] that controls cell cycle, apoptotic, and metabolic processes and supports effector differentiation.[36] However, IL-2R signaling seems to play a specific role in regulating proliferation and cell death in cTregs since pathways involved in these processes are all enhanced (Figure 2D). Indeed, the overall survival effect of IL-2[1,10] may predominately occur during the cTreg stage.

It seems paradoxical that proliferation pathways are upregulated in CD25^{iKO} cTregs, considering their lack of survival. Nevertheless, Ly6C^{+} and CD62L^{hi} cTregs have the largest fold-increase of Ki67 (Figures 2E and 2F). This result is consistent with the pathway data that the cTreg cell cycle is disproportionately regulated by IL-2 signaling and that this increased proliferation does not compensate for the overall survival defect in Tregs that lack CD25.[1,10] Since high levels of proliferation are characteristic of eTregs,[11] the high levels of proliferation in CD25^{iKO} cTregs may also reflect an adoption of eTreg characteristics, suggesting a possible role for IL-2 as a Treg checkpoint. Enhanced proliferation was also noted for CD25^{iKO} CD62L^{lo} Tregs (Figures 2E and 2F) and other eTregs subsets (CD119^{hi}, PD1^{hi}, ICOS^{hi}) (Figure S2D), but this increase was lower than that seen for CD25^{iKO} cTregs. Thus, the increased representation of eTregs after ablation of CD25 (Figure 1J) is unlikely to be fully accounted for by this enhanced proliferation.

IL-2R signaling influences the proportion of cTreg and eTreg subsets

The heterogeneity within cTregs or eTreg subsets[37] was not accounted for in our RNA-seq studies because they were sorted based solely on CD62L^{hi} and CD62L^{lo} expression, respectively. Thus, we performed scRNA-seq on total splenic Tregs isolated from CD25^{iKO} and CD25^{WT} mice. Approximately the same number of Tregs were sequenced for each genotype (Figure S3A). UMAP analysis of the entire Treg pool (CD25^{iKO} and CD25^{WT} combined) yielded six distinct clusters, two associated with cTregs and four with eTregs, where a shift toward eTreg subsets was noted (Figures 3A and S3B). These six clusters and their cluster-defining genes (Figure S3C) closely align with previously published scRNA-seq of WT splenic Tregs.[37]

Upon ablation of CD25, CD62L^{hi} cTregs were underrepresented compared to ICOS^{hi} eTregs (Figure 3B). Indeed, the proportion of cells in cTreg1 decreased and eTreg clusters 1–4 increased in CD25^{iKO} (Figures 3C and S3D). Cells in eTreg4 were disproportionately enriched after

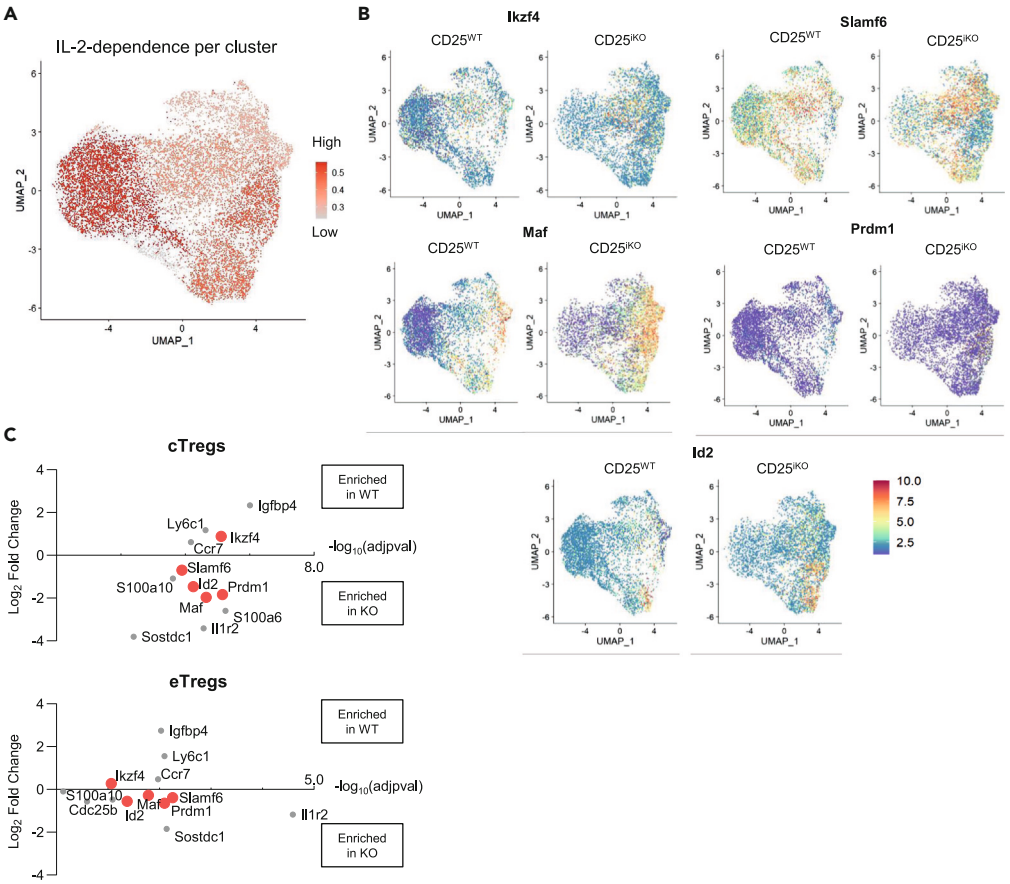

Figure 4. IL-2R signaling regulates molecular drivers of eTreg subsets

(A) IL-2-dependent genes determined by RNA-seq in Figure 2A were compared to cluster defining genes from scRNA-seq. The proportion of cluster-defining genes that are IL-2-dependent are plotted by color and overlayed onto the merged UMAP from Figure 3A with $CD25^{iKO}$ and $CD25^{WT}$ Tregs combined.

(B) UMAP feature plots of scRNA-seq data highlighting cluster-defining transcription factors that are IL-2-dependent.

(C) Transcription factors that define clusters in Figure 3 are shown by their fold change in cTregs (top) and eTreg (bottom).

loss of IL-2R signaling, a cluster that expresses *IFNγR1* and *Prdm1* (Figure 3D). This finding suggests that IL-2 normally restrains the abundance of cells in eTreg4 or that these cells are less dependent on IL-2 for their persistence. Furthermore, fewer cells from $CD25^{iKO}$ mice in the cTreg2 expressed genes characteristic of cTregs and acquired eTreg3 genes, such as *Id2, S100a4* and *Ccr2* (Figure 3D). The acquisition of effector genes in $CD25^{iKO}$ cTreg2 further implies that IL-2R signaling normally restrains Treg differentiation.

The eTreg2 cluster contains cells expressing *Bcl6*, *Pdcd1* and *Cxcr5*, which are characteristic of T follicular regulatory (T_{FR}) cells (Figures 3D and S4A).[21] T_{FR} have previously been shown to differentiate in the absence of IL-2 signaling, which we confirmed for the spleen from $CD25^{iKO}$ mice (Figure S4B).[29] Sclerostin domain-containing protein 1 (*Sostdc1*) and *Il1r2* in the eTreg2 cluster were among the most IL-2 dependent transcripts (Figures 4C and S4A). Sostdc1 is secreted by T_{FH}[38] cells to promote T_{FR} differentiation. Therefore, its expression in T_{FR} cells may reinforce further T_{FR} cell development. Il1r2 is a decoy receptor that neutralizes IL-1β[39] and its expression enhances T_{FR} cell suppressive activity to dampen available IL-1β which is necessary for T_{FH} cell activation.[40] Since IL-2 antagonizes differentiation of T_{FR} cells based on our studies (Figure S4) and others,[29] these genes are components of the T_{FR} program that are inhibited by IL-2.

IL-2R signaling regulates molecular drivers of eTreg subsets

Multiple transcripts that define the clusters identified by scRNA-seq were found to be differentially expressed by IL-2 in bulk RNA-seq studies, demonstrating the extent to which IL-2 defines the transcriptional program of Treg clusters (Figure 4A). The proportion of cluster-defining genes that are IL-2R-dependent is highest in the cTreg1 cluster, with eTreg3 and eTreg4 also dependent on IL-2R signaling (Figure 4A). Given this disproportionate influence of IL-2 on the transcriptional landscape, we hypothesized that IL-2 may regulate factors that are known to drive differentiation of specific eTregs. *Ikzf4 (EOS), Slamf6, Maf, Prdm1*, and *Id2* were among the IL-2-dependent mediators defining eTreg clusters (Figure 4B), however their greatest fold change was seen in cTregs (Figure 4C). This finding suggests that these differentiation factors are regulated by IL-2R signaling at the cTreg stage to drive differentiation of specialized eTregs. *Ikzf4* normally supports Treg suppressive function and is decreased

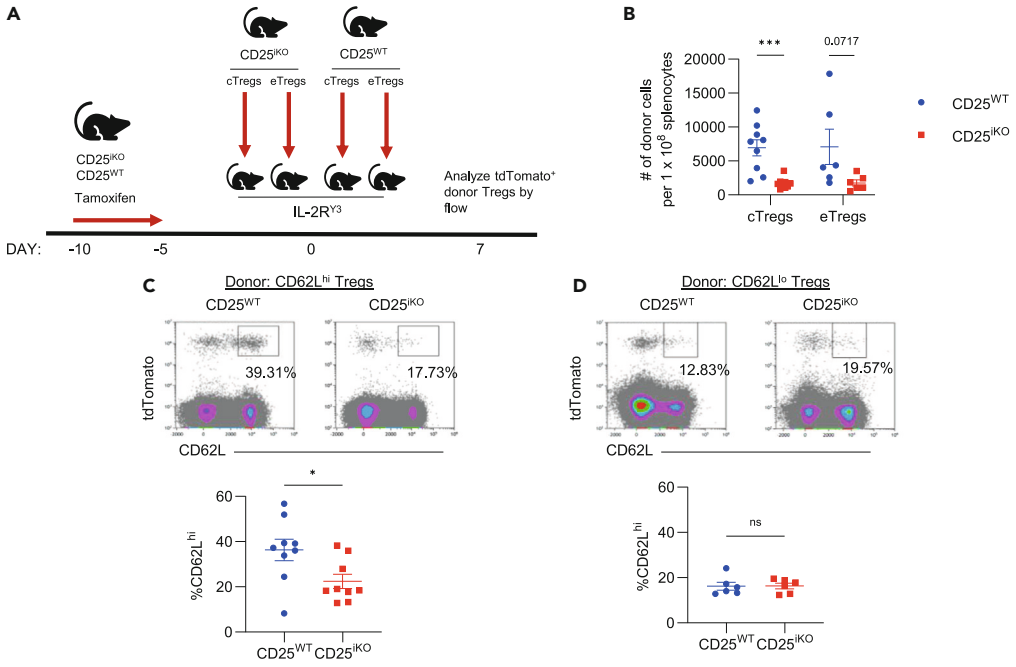

Figure 5. IL-2R signaling maintains Treg survival and the abundance of CD62L^{hi} cTregs

(A) Schematic of adoptive transfer of Treg subsets into IL-2Rβ mutant mice (IL-2Rβ^{Y3}). CD25^{WT} and CD25^{iKO} mice were treated with tamoxifen for five days (Day −10 to −5). Five days later (Day 0), CD25^{WT} and CD25^{iKO} CD62L^{hi} cTregs and CD62L^{lo} eTregs were FACS-sorted from the spleens and lymph nodes and 300,000 cells were adoptively transferred to IL-2Rβ^{Y3} recipient mice.

(B) 7 days post-transfer, the number of donor Tregs in the spleen of IL-2Rβ^{Y3} recipients were enumerated based on expression of the tdTomato-reporter.

(C) Representative flow cytometry dot plots (top) and quantitative data (bottom) of donor CD62L^{hi} tdTomato^{+} Tregs after gating CD4^{+} splenocytes 7 days post-transfer of cTregs.

(D) Representative flow cytometry dot plots (top) and quantitative data (bottom) of donor CD62L^{hi} tdTomato^{+} Tregs after gating CD4^{+} splenocytes 7 days post-transfer of eTregs. The percent in the dot plots (C, D) represents the fraction of donor Tregs that express CD62L. Data (n = 6–9) for (B) and (C) from 2 to 3 replicate experiments were analyzed by unpaired t tests. *$p < 0.05$, **$p < 0.01$, ***$p < 0.001$.

in CD25^{iKO} Tregs.[41] Signaling lymphocyte activation molecular family member 6 (*Slamf6*) augments TCR activation.[42] A decrease in *Ikzf4* and elevation of *Slamf6* is consistent with enhanced TCR-driven differentiation of less suppressive Tregs, which is consistent with the Treg phenotype observed *in vivo* (Figures 4B and 4C). *Id2*, *Maf* and *Prdm1* are highly expressed in eTregs and each are recognized to control unique aspects of eTreg differentiation[16,43,44] (Figure 4B). For example, the CD25^{iKO} eTreg4 subset is marked by high expression of *Maf* and *Prdm1*, which regulate the production of IL-10[45] (Figure 4B). *Maf* is also critical for differentiation of RORγt-expressing Tregs[26] and T_{FR} cells[44] (Figure 4B). *Id2* links TCR signaling to eTreg activation and is associated with less suppressive Tregs.[43] Its upregulation in eTreg3 and eTreg4 CD25^{iKO} could lead to the lack of suppressive function seen in CD25^{iKO}, despite their enhanced eTreg characteristics. Overall, multiple molecular drivers of eTreg subsets are restrained by IL-2R signaling and their upregulation is likely to promote the phenotypic changes observed in CD25^{iKO} Tregs.

IL-2R signaling maintains Treg survival and the abundance of CD62L^{hi} cTregs

Given the length of time between tamoxifen treatment and data collection, it is difficult to follow how specific populations of Tregs change after loss of IL-2R signaling. Therefore, adoptive transfer studies were performed to directly evaluate the role of IL-2R signaling in the differentiation of CD62L^{hi} cTregs and CD62L^{lo} eTregs. Each subset was purified from CD25^{WT} and CD25^{iKO} mice five days post-tamoxifen, then adoptively transferred into IL-2R^{Y3} mice, which bear mutations in 3 key tyrosine residues within the cytoplasmic tail of IL-2Rβ. These mutations allow for reduced competition between donor and host Tregs that leads to improved engraftment of donor cells (Figure 5A).

Seven days post-transfer, the persistence and differentiation of donor cTregs and eTregs were evaluated. Donor CD25^{iKO} Tregs were less abundant than WT counterparts within spleens of recipient mice (Figure 5B). Thus, in line with other studies,[1,10] IL-2R signaling appears to be required for survival of both cTregs and eTregs. When considering those Tregs that persisted, the development of CD62L^{lo} eTregs from donor CD62L^{hi} cTregs was enhanced in cells lacking CD25, again suggesting that IL-2R signaling may normally impede differentiation into eTregs (Figure 5C). When eTregs were transferred, a small fraction CD25^{WT} and CD25^{iKO} Tregs similarly reverted to CD62L^{hi} Tregs (Figure 5D). These data suggest IL-2R signaling not only maintains Treg survival but also restrains Treg differentiation from cTregs to eTregs.

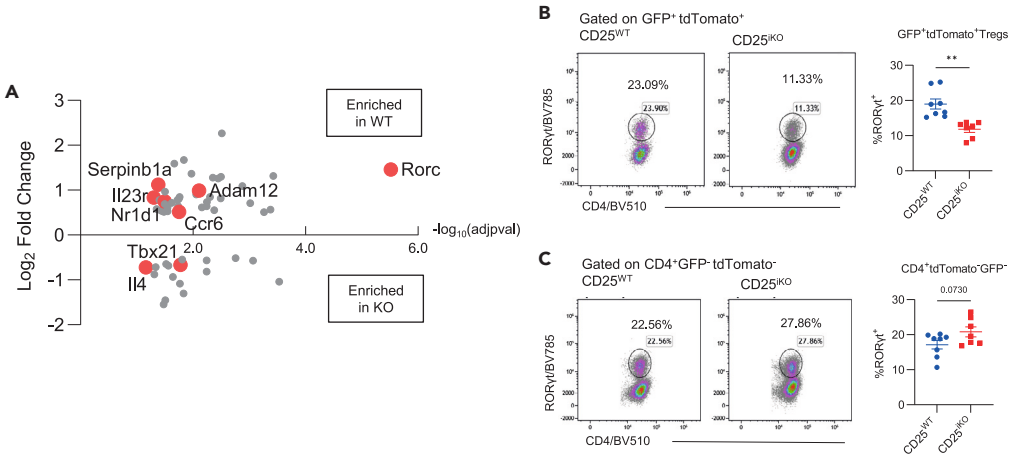

Figure 6. RORγt$^+$ Tregs depend on IL-2R signaling

(A) 58 IL-2 dependent genes unique to CD25^{iKO} eTregs with genes specific to T_H17 and/or T_R17 highlighted in red.

(B and C) CD25^{WT} and CD25^{iKO} mice were induced with tamoxifen for 5 days. 4 weeks later, lymphocytes were isolated from the small intestine lamina propria. Representative flow cytometry dot plots (left) and quantitative data (right) of RORγt expression by CD25^{WT} and CD25^{iKO} tdTomato$^+$ Tregs (B) or CD4$^+$ GFP$^-$ tdTomato$^-$ conventional T cells (C) Data (n = 7–8) from at least two replicate experiments were analyzed by an unpaired t-test. $^{**}p < 0.01$.

RORγt$^+$ Tregs depend on IL-2R signaling

Although our data indicate an important role of IL-2 in cTregs, we also found a significant impact of IL-2 in eTregs. To assess the specific contribution of IL-2R signaling in eTregs, we examined the 58 differentially expressed genes that are unique to eTregs relative to cTreg (Figures 2B and 6A). Several of these genes, including *Ccr6*, *Il23r* and *Rorc*, are characteristic of ICOS^{hi} CCR6$^+$ RORγt$^+$ Tregs, or otherwise recognized as T_R17 cells.[24] Moreover *Adam12*, *SerpinB1*, and *Nr1d1* were also identified, and each have been implicated in regulation of conventional T_H17 cells, raising the possibility of an analogous role in T_R17 cells.[46–48] Remarkably, all these genes were downregulated in eTregs from CD25^{iKO} mice (Figure 6A). Furthermore, genes involved with inhibition of the T_H17 program, such as *Il4* and *Tbx21*, were increased.[49,50]

Given that T_R17 cells are mainly found at mucosal and barrier sites, rather than secondary lymphoid tissues, we compared RORγt$^+$ Tregs in the small intestine lamina propria of CD25^{WT} and CD25^{iKO} mice at 4 weeks post-tamoxifen. We found that the frequency of RORγt$^+$ Tregs was significantly reduced in CD25^{iKO} mice (Figure 6B). No statistically significant difference in RORγt$^+$ conventional CD4$^+$ T cells was noted (Figure 6C). These data indicate a role for IL-2R signaling for the differentiation and/or maintenance of RORγt$^+$ Tregs that populate the small intestine lamina propria.

IL-2R signaling represses IFNγ immune signature associated with eTregs

After inducible knockout of CD25, eTregs proportionally increase (Figures 1J and 3C) but suppressive function is reduced (Figures 1G–1I), raising the possibility of Treg instability. IFNγ and its signaling factors have previously been shown to promote Treg instability.[51,52] *IFNγR1* defines cluster eTreg4, which was uniquely increased in spleens of CD25^{iKO} mice (Figure 7A), and surface IFNγR1 protein was also significantly increased in CD25^{iKO} Tregs compared to WT controls (Figure 7B). This finding suggests that impaired IL-2R signaling may lead to increased IFNγ signaling in CD25^{iKO} Tregs due to increased IFNγR1 expression. Accordingly, the Interferon Gamma Response pathway was significantly enriched in CD25^{iKO} Tregs compared to WT counterparts (Figure 2D). Genes within this pathway show a central set of genes that are increased in the absence of CD25 usually in both cTregs and eTregs, including *Hif1α*, *Jak2*, *Irf4*, *Vcam1*, *Ifitm2*, and *Ifngr1* (Figure 7C). *Socs1*, a negative regulator of IFNγ signaling that is induced by IFNγ, was downregulated in the absence of CD25, suggesting that IL-2R signaling may restrain IFNγ signaling by upregulating *Socs1*.

IFNγ-secreting cells were measured in the mesenteric lymph node (MLN) and small intestine lamina propria to determine if more IFNγ was available to bind IFNγR1$^+$ Tregs found in CD25^{iKO} mice. There was an increase in IFNγ-producing CD4$^+$ conventional (Figures 7D and 7E) and CD8$^+$ T cells (Figures 7F and 7G) in the MLN and small intestine lamina propria in CD25^{iKO} mice. Furthermore, CD25^{iKO} Tregs themselves produce higher levels of IFNγ after *in vitro* stimulation, reflecting impaired stability (Figures 7H and 7I). Thus, impaired IL-2R signaling in Tregs leads to an increase in T_H1 autoreactive T cells and upregulation of an IFNγR1 expressing subset of Tregs, that may be destabilized by the increased availability of IFNγ.[51–53]

DISCUSSION

Although past studies show that IL-2 is essential for the survival, homeostasis, and function of cTregs and eTregs,[1,10] the specific role of IL-2R signaling in major Treg subsets remains poorly understood. By inducibly and selectively knocking out CD25 to inhibit IL-2R signaling in peripheral Tregs, we demonstrate the transcriptome of cTregs and eTregs, defined by high and low expression of CD62L, respectively, is altered

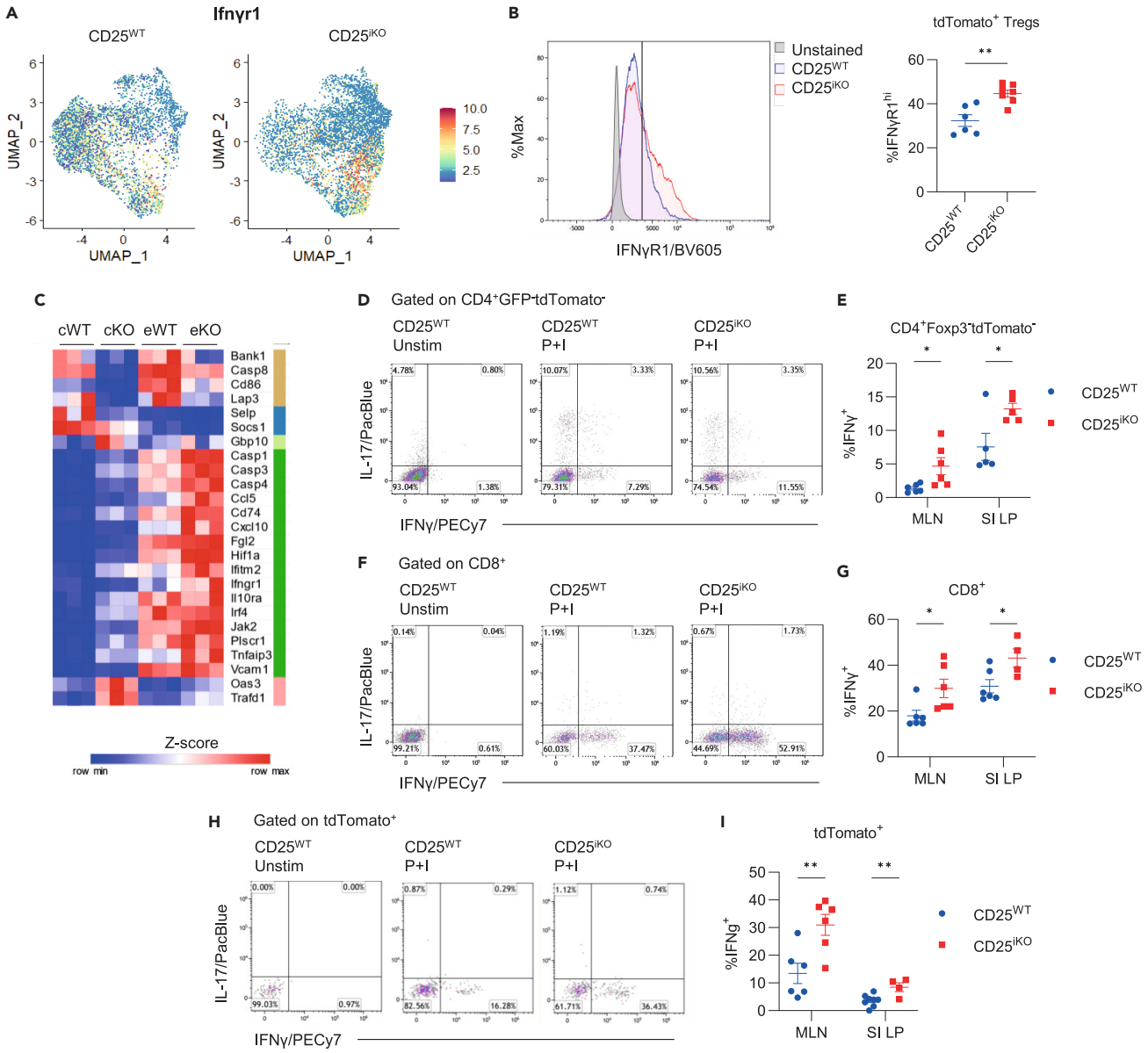

Figure 7. IL-2R signaling represses IFNγ immune signature associated with eTregs

(A) IFNγR1 expression overlayed on UMAP plots (Figure 4A), where transcript abundance is designated by color intensity for CD25^{WT} and CD25^{iKO} Tregs.

(B) Representative flow cytometry histogram (left) and quantitative data (right) of expression of IFNγR1 by CD25^{WT} and CD25^{iKO} Tregs.

(C) Heatmap of DEGs between CD25^{WT} and CD25^{iKO} splenic Treg subsets from the Hallmark Interferon Gamma Response pathway.

(D–I) CD25^{WT} and CD25^{iKO} mice were treated with tamoxifen. Four weeks later, lymphocytes from the MLN and small intestine lamina propria were cultured in the presence of Golgi inhibitors with and without PMA/Ionomycin for 4 h and the indicated cytokines were enumerated by intracellular FACS analysis. Representative flow cytometry dot plots from the lamina propria (D, F) or MLN (H) and quantitative data (E, G, I) for IFNγ-producing CD4$^+$ T conventional (E) and CD8$^+$ (G) T cells and tdTomato$^+$ Tregs (I). Data (n = 4–8) are from at least two replicate experiments were analyzed by unpaired t-test, *$p < 0.05$, **$p < 0.01$.

in both subsets, with cTregs being more substantially affected. This finding is consistent with past work that showed that a higher fraction of cTregs express the high affinity IL-2R and respond to IL-2 *in vivo* based on STAT5 activation.[13] Notably, as discussed more fully below, cTregs in CD25^{iKO} mice are not 'resting', as typically seen in normal mice, but are hyperproliferative while acquiring traits of eTregs.

Most of the CD25-dependent eTreg transcriptome overlaps in the same direction with the more numerous IL-2-dependent genes associated with cTregs. This finding indicates that there are a set of genes co-regulated by IL-2 in both subsets. This could happen by one of two mechanisms: (1) cTregs and eTregs directly respond to available IL-2 in their microenvironment or (2) IL-2 initially affects gene expression in cTregs, and these changes persist or are programmed into eTregs. We cannot discriminate between these possibilities. However,

programming in cTregs cannot fully account for all the transcriptome changes in eTregs because we identified a set of genes that are solely IL-2-dependent in eTregs. Some of these genes are associated with regulation of T_H17 and T_R17 cells.[24,46–48] These same genes decreased in $CD25^{iKO}$ eTregs and resulted in fewer T_R17 cells, which are also less functional at suppressing EAE.[10] This finding is distinct from the known role of IL-2 in opposing T_H17 development.[54] However, IFNγ is also known to inhibit the generation of T_H17 cells[49] and the elevated IFNγ in $CD25^{iKO}$ mice may have a role in preventing differentiation of T_R17.

IFNγR11 mRNA and protein also increased in a subset of eTregs, which enhances the capacity of these Tregs to respond to IFNγ. When eTregs sense IFNγ, they exhibit fragility that lowers their suppressive function.[51,52,55] Accordingly, Tregs, conventional $CD4^+$ and $CD8^+$ T cells from $CD25^{iKO}$ mice produced a heightened amount of IFNγ when re-challenged *in vitro*. This phenotype is consistent with the increase in autoreactive $CD4^+$ $PD1^+$ T cells and activated $CD62L^{lo}$ $CD44^{hi}$ conventional $CD4^+$ and $CD8^+$ T cells after inducible deletion of CD25 in Tregs. Therefore, the loss of IL-2R signaling predisposes Tregs to become fragilized, leading them to proliferate and differentiate to compensate for their reduced suppressive activity. Some of the unique changes in gene expression in eTregs likely support their development into specialized subsets of suppressive cells and/or to regulate their suppressive activity in response to T cell activation. During an immune response, Teff cells will utilize IL-2, which may make it less available for Tregs. This scenario could lead to increased expression of IFNγR1 on eTregs and responsiveness to IFNγ produced by Teff cells, which in turn lowers Treg suppressive function, to enhance an ongoing immune response. Another possibility is that impaired survival of Tregs after ablation of CD25 may also contribute to lower suppressive function.

Many studies show that IL-2 acts in concert with TCR and co-stimulatory signaling to drive the expansion of Tregs *in vitro*.[56] In addition, treatment of mice and humans with low-dose IL-2 or IL-2 analogs leads to Treg proliferation and expansion *in vivo*.[57,58] Therefore, a highly unexpected results was that deletion of CD25 in Tregs resulted in hyper, rather than reduced, proliferation, with cTregs showing the greatest fold increase. Our findings, combined with those showing that administering IL-2 supports Treg expansion *in vivo*, indicate that IL-2R signaling appears to behave as a checkpoint that finely tunes responses of cTregs. Within a moderate range, the growth and survival activity of IL-2R signaling are balanced and cTregs are maintained at a homeostatic number. When IL-2 is reduced or excessive, Tregs show enhanced proliferation.

The increased proliferation by cTregs to impaired IL-2R signaling does not lead to an accumulation of cTregs. Rather, cTregs are selectively reduced when compared to eTregs. This likely reflects that cTreg survival is impaired, leading to cell death, and that other cTregs differentiate into eTregs. Supporting these conclusions, pathway analysis indicates that although proliferation increases, cell death is also enhanced and pro-survival Bcl2 is reduced in $CD25^{iKO}$ cTregs. Moreover, scRNAseq also revealed that the more differentiated cTreg2 subset acquired traits of eTregs because of impaired IL-2R signaling. The high sharing of IL-2-dependent transcripts for cTregs and eTregs raises the possibility that eTregs may be at least in part programmed as cTregs. Indeed, many transcripts (Figures 3D and 4C) that are highly expressed in eTregs were upregulated in $CD25^{iKO}$ cTregs, including transcription factors such as Prdm-1, Id2 and Maf with known roles in promoting eTregs.[16,43,44] Adoptive transfer of $CD25^{iKO}$ Tregs revealed a composite of these properties, i.e., poor survival, but for the donor cTregs that persist, they more readily developed into eTregs than $CD25^{WT}$ cTregs. These data suggest that that some portion of cTregs adopt an eTreg phenotype upon loss of IL-2R signaling.

These types of effects may have important implications in how Tregs maintain tolerance (Figure 8). Under normal homeostatic conditions, IL-2 from autoreactive T cells supports cTregs in peripheral lymph nodes which in turn suppress autoreactive T cells.[9] However, when this balance is altered to favor autoreactive T cells, these cells may more favorably compete for IL-2 and become activated, which in turn lowers available IL-2 for cTregs. This type of reduction in IL-2 might support proliferation and differentiation of cTregs into eTregs, which match their suppressive function to activate autoreactive T cells. As such, the sensing of IL-2 by cTregs may function as a checkpoint. Indeed, this scenario is highly analogous to what occurred in the spleen after ablation of CD25 expression for Tregs. We noted an increase in activated autoreactive T cells while cTregs declined and eTregs became more numerous. However, the suppressive activity of these cells was reduced, despite their effector phenotype, indicating that IL-2 signaling is needed to support the suppressive function of eTregs.

In conclusion, a dominant effect of loss of IL-2R signaling by thymic-derived Tregs after seeding the periphery is impaired survival.[1,10] However, this survival effect takes a considerable time (3–4 months) to completely unfold. This allowed assessment of the consequence of the loss of IL-2R signaling on the two major Treg subsets based on high and low expression of CD62L. These data and those from previous studies where Tregs are stimulated by exogenous IL-2 provide a new picture that under both circumstances Treg proliferation results. In this light, IL-2 acts as a checkpoint to control the balance and function of Treg subsets. Under homeostatic conditions, cTregs with high CD25 expression sequester IL-2 from autoreactive T cells to maintain tolerance and restrain eTreg differentiation (Figure 8). When self-reactive T cells become activated, they have increased capacity to bind IL-2 through the upregulation of CD25. This shifts IL-2 utilization to activated T cells and reduces IL-2R signaling in cTregs to favor differentiation into specialized suppressors with enhanced ability to respond to specific inflammatory programs. Under other circumstances where IL-2R signaling is further reduced, Treg instability may be induced through increased sensitivity to IFNγ and lower Foxp3 expression to limit a Treg functional response and promote continued inflammation. These results, as discussed above, have implications concerning how IL-2 contributes to Treg tolerance beyond promoting thymic Treg development and the consequences of Treg-directed IL-2 as therapy for autoimmunity.

Limitations of the study

One limitation to these studies is the amount of time between tamoxifen treatment and data collection, which makes it difficult to pinpoint exactly how Treg subsets are shifting. For example, cTregs have the highest levels of proliferation, yet eTregs also increase proliferation in

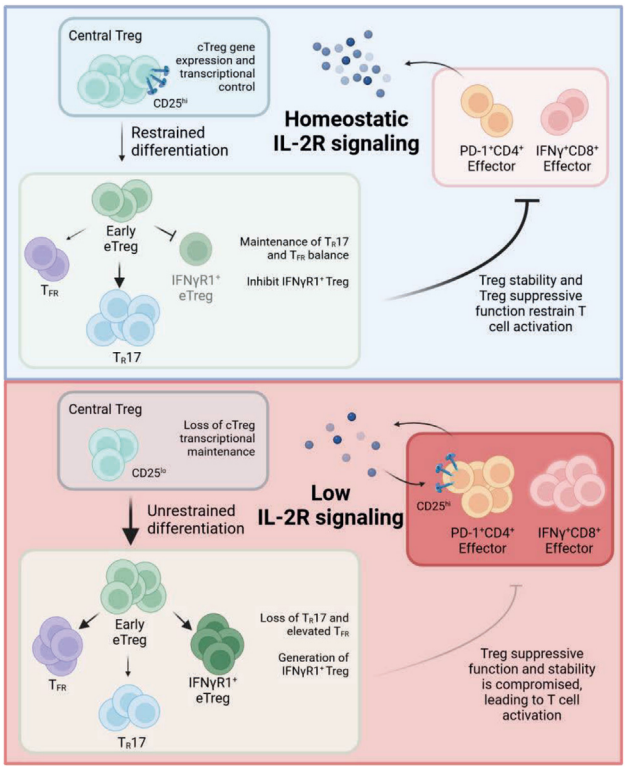

Figure 8. Post-thymic IL-2R signaling is required for Treg subset maintenance, stability and self-tolerance

Homeostatic IL-2R signaling maintains cTreg transcriptional programs and regulates the balance between T_{FR}, T_R17 and other eTregs. Under low IL-2R signaling, the cTreg transcriptional program is lost and cTregs differentiate more readily into eTregs. T_R17 differentiation is inhibited and other eTregs become more abundant. IFNγR1$^+$ Tregs are generated and Tregs suppressive function is compromised, leading to a T_H1-type inflammatory response.

response to CD25^{iKO}, indicating that some of these eTregs may expand and compensate for the reduction of more IL-2-dependent Treg cells. However, adoptive transfer studies, which isolate specific populations, illustrate the comparable survival defect between cTregs and eTregs and the increased differentiation in adoptively transferred CD25^{iKO} cTregs. Another limitation is that we have not directly addressed the extent that eTregs are programmed at the level of cTregs. We believe that this is an important area for future study that may help to better understand the mechanism by which the development of eTregs is regulated.

RESOURCE AVAILABILITY

Lead contact

Further information and requests should be directed to the lead contact, Thomas Malek (tmalek@med.miami.edu).

Materials availability

This study did not generate unique materials.

Data and code availability

- The RNA-seq and the scRNA-seq data can be accessed through NCBI: GSE268024.
- This article does not report original code.
- Other data will be made available upon reasonable request by the lead contact.

ACKNOWLEDGMENTS

This work was supported by the NIH R01AI148675 (to T.R.M.) and F30AI157211 (to A.N.S.). NIH T32GM145462 also supported A.N.S. Oliver Umland at the Diabetes Research Institute Flow Cytometry Core provided expertise in flow cytometry and cell sorting. Natalia Arenas contributed technical expertise. The Oncogenomics Shared Resource at the Sylvester Comprehensive Cancer Center (supported by NIH P30CA240139) conducted the sequencing for these studies.

AUTHOR CONTRIBUTIONS

Conception and design: T.R.M. and A.N.S.; performed experiments, A.N.S.; analysis and interpretation of data, A.N.S., A.V.V., and T.R.M.; manuscript writing, A.N.S. and T.R.M.; all authors edited and approved the manuscript.

DECLARATION OF INTERESTS

The University of Miami and Thomas Malek have a patent on IL-2/CD25 fusion proteins and this technology has been licensed to Bristol Myers Squibb by the University of Miami for commercial development. Both receive royalties for its commercialization.

STAR★METHODS

Detailed methods are provided in the online version of this paper and include the following:

- KEY RESOURCES TABLE
- EXPERIMENTAL MODEL AND STUDY PARTICIPANT DETAILS
- METHOD DETAILS
  - Lymphocyte isolation
  - Flow cytometry and FACS
  - Adoptive transfer
  - Single Cell RNA-seq
  - RNA-seq
  - Cytokine staining
- QUANTIFICATION AND STATISTICAL ANALYSIS

SUPPLEMENTAL INFORMATION

Supplemental information can be found online at https://doi.org/10.1016/j.isci.2024.111248.

Received: May 29, 2024
Revised: September 24, 2024
Accepted: October 22, 2024
Published: October 24, 2024

REFERENCES

1. Toomer, K.H., Lui, J.B., Altman, N.H., Ban, Y., Chen, X., and Malek, T.R. (2019). Essential and non-overlapping IL-2Rα-dependent processes for thymic development and peripheral homeostasis of regulatory T cells. Nat. Commun. *10*, 1037.
2. Chinen, T., Kannan, A.K., Levine, A.G., Fan, X., Klein, U., Zheng, Y., Gasteiger, G., Feng, Y., Fontenot, J.D., and Rudensky, A.Y. (2016). An essential role for the IL-2 receptor in Treg cell function. Nat. Immunol. *17*, 1322–1333.
3. Fontenot, J.D., Rasmussen, J.P., Gavin, M.A., and Rudensky, A.Y. (2005). A function for interleukin 2 in Foxp3-expressing regulatory T cells. Nat. Immunol. *6*, 1142–1151.
4. Shouse, A.N., LaPorte, K.M., and Malek, T.R. (2024). Interleukin-2 signaling in the regulation of T cell biology in autoimmunity and cancer. Immunity *57*, 414–428.
5. Marshall, D., Sinclair, C., Tung, S., and Seddon, B. (2014). Differential requirement for IL-2 and IL-15 during bifurcated development of thymic regulatory T cells. J. Immunol. *193*, 5525–5533.
6. Weist, B.M., Kurd, N., Boussier, J., Chan, S.W., and Robey, E.A. (2015). Thymic regulatory T cell niche size is dictated by limiting IL-2 from antigen-bearing dendritic cells and feedback competition. Nat. Immunol. *16*, 635–641.
7. Vang, K.B., Yang, J., Mahmud, S.A., Burchill, M.A., Vegoe, A.L., and Farrar, M.A. (2008). IL-2, -7, and -15, but Not Thymic Stromal Lymphopoeitin, Redundantly govern $CD4^+Foxp3^+$ regulatory T cell development. J. Immunol. *181*, 3285–3290.
8. Malek, T.R., Yu, A., Vincek, V., Scibelli, P., and Kong, L. (2002). CD4 regulatory T cells prevent lethal autoimmunity in IL-2Rβ-deficient mice. Implications for the nonredundant function of IL-2. Immunity *17*, 167–178.
9. Wong, H.S., Park, K., Gola, A., Baptista, A.P., Miller, C.H., Deep, D., Lou, M., Boyd, L.F., Rudensky, A.Y., Savage, P.A., et al. (2021). A local regulatory T cell feedback circuit maintains immune homeostasis by pruning self-activated T cells. Cell *184*, 3981–3997.e22.
10. Fan, M.Y., Low, J.S., Tanimine, N., Finn, K.K., Priyadharshini, B., Germana, S.K., Kaech, S.M., and Turka, L.A. (2018). Differential roles of il-2 signaling in developing versus mature Tregs. Cell Rep. *25*, 1204–1213.e4.
11. Toomer, K.H., Yuan, X., Yang, J., Dee, M.J., Yu, A., and Malek, T.R. (2016). Developmental progression and interrelationship of central and effector regulatory T cell subsets. J. Immunol. *196*, 3665–3676.
12. Liston, A., and Gray, D.H.D. (2014). Homeostatic control of regulatory T cell diversity. Nat. Rev. Immunol. *14*, 154–165.
13. Smigiel, K.S., Richards, E., Srivastava, S., Thomas, K.R., Dudda, J.C., Klonowski, K.D., and Campbell, D.J. (2014). CCR7 provides localized access to IL-2 and defines homeostatically distinct regulatory T cell subsets. J. Exp. Med. *211*, 121–136.
14. Burton, O.T., Bricard, O., Tareen, S., Gergelits, V., Andrews, S., Biggins, L., Roca, C.P., Whyte, C., Junius, S., Brajic, A., et al. (2024). The tissue-resident regulatory T cell pool is shaped by transient multi-tissue migration and a conserved residency program. Immunity *57*, 1586–1602.e10.
15. Levine, A.G., Arvey, A., Jin, W., and Rudensky, A.Y. (2014). Continuous requirement for the TCR in regulatory T cell function. Nat. Immunol. *15*, 1070–1078.
16. Cretney, E., Xin, A., Shi, W., Minnich, M., Masson, F., Miasari, M., Belz, G.T., Smyth, G.K., Busslinger, M., Nutt, S.L., and Kallies, A. (2011). The transcription factors Blimp-1 and IRF4 jointly control the differentiation and function of effector regulatory T cells. Nat. Immunol. *12*, 304–311.
17. Koizumi, S.I., and Ishikawa, H. (2019). Transcriptional Regulation of differentiation and functions of effector T regulatory cells. Cells *8*, 939.
18. DiSpirito, J.R., Zemmour, D., Ramanan, D., Cho, J., Zilionis, R., Klein, A.M., Benoist, C., and Mathis, D. (2018). Molecular diversification of regulatory T cells in nonlymphoid tissues. Sci. Immunol. *3*, eaat5861.
19. Zheng, Y., Chaudhry, A., Kas, A., deRoos, P., Kim, J.M., Chu, T.T., Corcoran, L., Treuting, P., Klein, U., and Rudensky, A.Y. (2009). Regulatory T-cell suppressor program co-opts transcription factor IRF4 to control TH2 responses. Nature *458*, 351–356.
20. Koch, M.A., Tucker-Heard, G., Perdue, N.R., Killebrew, J.R., Urdahl, K.B., and Campbell, D.J. (2009). The transcription factor T-bet controls regulatory T cell homeostasis and function during type 1 inflammation. Nat. Immunol. *10*, 595–602.
21. Chung, Y., Tanaka, S., Chu, F., Nurieva, R.I., Martinez, G.J., Rawal, S., Wang, Y.H., Lim, H., Reynolds, J.M., Zhou, X.h., et al. (2011). Follicular regulatory T cells expressing Foxp3

and Bcl-6 suppress germinal center reactions. Nat. Med. *17*, 983–988.
22. Lu, Y., and Craft, J. (2021). Follicular Regulatory Cells: Choreographers of productive germinal center responses. Front. Immunol. *12*, 679909.
23. Linterman, M.A., Pierson, W., Lee, S.K., Kallies, A., Kawamoto, S., Rayner, T.F., Srivastava, M., Divekar, D.P., Beaton, L., Hogan, J.J., et al. (2011). Foxp3^{+} follicular regulatory T cells control the germinal center response. Nat. Med. *17*, 975–982.
24. Kim, B.-S., Lu, H., Ichiyama, K., Chen, X., Zhang, Y.B., Mistry, N.A., Tanaka, K., Lee, Y.H., Nurieva, R., Zhang, L., et al. (2017). Generation of RORγt+ antigen-specific T regulatory 17 cells from Foxp3+ precursors in autoimmunity. Cell Rep. *21*, 195–207.
25. Yang, B.-H., Hagemann, S., Mamareli, P., Lauer, U., Hoffmann, U., Beckstette, M., Föhse, L., Prinz, I., Pezoldt, J., Suerbaum, S., et al. (2016). Foxp3^{+} T cells expressing RORγt represent a stable regulatory T-cell effector lineage with enhanced suppressive capacity during intestinal inflammation. Mucosal Immunol. *9*, 444–457.
26. Xu, M., Pokrovskii, M., Ding, Y., Yi, R., Au, C., Harrison, O.J., Galan, C., Belkaid, Y., Bonneau, R., and Littman, D.R. (2018). c-MAF-dependent regulatory T cells mediate immunological tolerance to a gut pathobiont. Nature *554*, 373–377.
27. Hanna, B.S., Wang, G., Galván-Peña, S., Mann, A.O., Ramirez, R.N., Muñoz-Rojas, A.R., Smith, K., Wan, M., Benoist, C., and Mathis, D. (2023). The gut microbiota promotes distal tissue regeneration via RORγ^{+} regulatory T cell emissaries. Immunity *56*, 829–846.e8.
28. Furuyama, K., Kondo, Y., Shimizu, M., Yokosawa, M., Segawa, S., Iizuka, A., Tanimura, R., Tsuboi, H., Matsumoto, I., and Sumida, T. (2022). RORγt^{+}Foxp3^{+} regulatory T cells in the regulation of autoimmune arthritis. Clin. Exp. Immunol. *207*, 176–187.
29. Botta, D., Fuller, M.J., Marquez-Lago, T.T., Bachus, H., Bradley, J.E., Weinmann, A.S., Zajac, A.J., Randall, T.D., Lund, F.E., León, B., and Ballesteros-Tato, A. (2017). Dynamic regulation of T follicular regulatory cell responses by interleukin 2 during influenza infection. Nat. Immunol. *18*, 1249–1260.
30. Cheng, G., Yuan, X., Tsai, M.S., Podack, E.R., Yu, A., and Malek, T.R. (2012). IL-2 receptor signaling is essential for the development of Klrg1+ terminally differentiated T regulatory cells. J. Immunol. *189*, 1780–1791.
31. Rubtsov, Y.P., Niec, R.E., Josefowicz, S., Li, L., Darce, J., Mathis, D., Benoist, C., and Rudensky, A.Y. (2010). Stability of the regulatory t cell lineage *in vivo*. Science *329*, 1667–1671.
32. Madisen, L., Zwingman, T.A., Sunkin, S.M., Oh, S.W., Zariwala, H.A., Gu, H., Ng, L.L., Palmiter, R.D., Hawrylycz, M.J., Jones, A.R., et al. (2010). A robust and high-throughput Cre reporting and characterization system for the whole mouse brain. Nat. Neurosci. *13*, 133–140.
33. Pearce, E.L., Mullen, A.C., Martins, G.A., Krawczyk, C.M., Hutchins, A.S., Zediak, V.P., Banica, M., DiCioccio, C.B., Gross, D.A., Mao, C.A., et al. (2003). Control of effector CD8 $^{+}$ T cell function by the transcription factor *eomesodermin*. Science *302*, 1041–1043.
34. Preston, G.C., Sinclair, L.V., Kaskar, A., Hukelmann, J.L., Navarro, M.N., Ferrero, I., MacDonald, H.R., Cowling, V.H., and Cantrell, D.A. (2015). Single cell tuning of Myc expression by antigen receptor signal strength and interleukin-2 in T lymphocytes. EMBO J. *34*, 2008–2024.
35. Villarino, A.V., Laurence, A.D., Davis, F.P., Nivelo, L., Brooks, S.R., Sun, H.W., Jiang, K., Afzali, B., Frasca, D., Hennighausen, L., et al. (2022). A central role for STAT5 in the transcriptional programing of T helper cell metabolism. Sci. Immunol. *7*, eabl9467.
36. Wang, R., Dillon, C.P., Shi, L.Z., Milasta, S., Carter, R., Finkelstein, D., McCormick, L.L., Fitzgerald, P., Chi, H., Munger, J., and Green, D.R. (2011). The transcription factor Myc controls metabolic reprogramming upon T lymphocyte activation. Immunity *35*, 871–882.
37. Zemmour, D., Zilionis, R., Kiner, E., Klein, A.M., Mathis, D., and Benoist, C. (2018). Single-cell gene expression reveals a landscape of regulatory T cell phenotypes shaped by the TCR. Nat. Immunol. *19*, 291–301.
38. Wu, X., Wang, Y., Huang, R., Gai, Q., Liu, H., Shi, M., Zhang, X., Zuo, Y., Chen, L., Zhao, Q., et al. (2020). SOSTDC1-producing follicular helper T cells promote regulatory follicular T cell differentiation. Science *369*, 984–988.
39. Mercer, F., Kozhaya, L., and Unutmaz, D. (2010). Expression and function of TNF and IL-1 receptors on human regulatory T cells. PLoS One *5*, e8639.
40. Ritvo, P.-G.G., Churlaud, G., Quiniou, V., Florez, L., Brimaud, F., Fourcade, G., Mariotti-Ferrandiz, E., and Klatzmann, D. (2017). T $_{fr}$ cells lack IL-2Rα but express decoy IL-1R2 and IL-1Ra and suppress the IL-1–dependent activation of T $_{fh}$ cells. Sci. Immunol. *2*, eaan0368.
41. Gokhale, A.S., Gangaplara, A., Lopez-Occasio, M., Thornton, A.M., and Shevach, E.M. (2019). Selective deletion of Eos (Ikzf4) in T-regulatory cells leads to loss of suppressive function and development of systemic autoimmunity. J. Autoimmun. *105*, 102300.
42. Gartshteyn, Y., Askanase, A.D., Song, R., Bukhari, S., Dragovich, M., Adam, K., and Mor, A. (2023). SLAMF6 compartmentalization enhances T cell functions. Life Sci. Alliance *6*, e202201533.
43. Han, X., Huang, H., Gao, P., Zhang, Q., Liu, X., Jia, B., Strober, W., Hou, B., Zhou, X., Gao, G.F., and Zhang, F. (2019). E-protein regulatory network links TCR signaling to effector Treg cell differentiation. Proc. Natl. Acad. Sci. USA *116*, 4471–4480.
44. Wheaton, J.D., Yeh, C.-H., and Ciofani, M. (2017). Cutting Edge: c-Maf is required for regulatory T cells to adopt RORγt^{+} and follicular phenotypes. J. Immunol. *199*, 3931–3936.
45. Gabryšová, L., Alvarez-Martinez, M., Luisier, R., Cox, L.S., Sodenkamp, J., Hosking, C., Pérez-Mazliah, D., Whicher, C., Kannan, Y., Potempa, K., et al. (2018). c-Maf controls immune responses by regulating disease-specific gene networks and repressing IL-2 in CD4^{+} T cells. Nat. Immunol. *19*, 497–507.
46. Zhou, A.X., El Hed, A., Mercer, F., Kozhaya, L., and Unutmaz, D. (2013). The metalloprotease ADAM12 regulates the effector function of human Th17 cells. PLoS One *8*, e81146.
47. Hou, L., and Yuki, K. (2020). SerpinB1 expression in Th17 cells depends on hypoxia-inducible factor 1-alpha. Int. Immunopharm. *87*, 106826.
48. Amir, M., Chaudhari, S., Wang, R., Campbell, S., Mosure, S.A., Chopp, L.B., Lu, Q., Shang, J., Pelletier, O.B., He, Y., et al. (2018). REV-ERBα regulates TH17 cell development and autoimmunity. Cell Rep. *25*, 3733–3749.e8.
49. Harrington, L.E., Hatton, R.D., Mangan, P.R., Turner, H., Murphy, T.L., Murphy, K.M., and Weaver, C.T. (2005). Interleukin 17–producing CD4^{+} effector T cells develop via a lineage distinct from the T helper type 1 and 2 lineages. Nat. Immunol. *6*, 1123–1132.
50. Lazarevic, V., Chen, X., Shim, J.H., Hwang, E.S., Jang, E., Bolm, A.N., Oukka, M., Kuchroo, V.K., and Glimcher, L.H. (2011). T-bet represses TH17 differentiation by preventing Runx1-mediated activation of the gene encoding RORγt. Nat. Immunol. *12*, 96–104.
51. Srivastava, S., Koch, M.A., Pepper, M., and Campbell, D.J. (2014). Type I interferons directly inhibit regulatory T cells to allow optimal antiviral T cell responses during acute LCMV infection. J. Exp. Med. *211*, 961–974.
52. Gangaplara, A., Martens, C., Dahlstrom, E., Metidji, A., Gokhale, A.S., Glass, D.D., Lopez-Ocasio, M., Baur, R., Kanakabandi, K., Porcella, S.F., and Shevach, E.M. (2018). Type I interferon signaling attenuates regulatory T cell function in viral infection and in the tumor microenvironment. PLoS Pathog. *14*, e1006985.
53. Overacre-Delgoffe, A.E., Chikina, M., Dadey, R.E., Yano, H., Brunazzi, E.A., Shayan, G., Horne, W., Moskovitz, J.M., Kolls, J.K., Sander, C., et al. (2017). Interferon-γ drives Treg fragility to promote anti-tumor immunity. Cell *169*, 1130–1141.e11.
54. Laurence, A., Tato, C.M., Davidson, T.S., Kanno, Y., Chen, Z., Yao, Z., Blank, R.B., Meylan, F., Siegel, R., Hennighausen, L., et al. (2007). Interleukin-2 Ssgnaling via STAT5 constrains T helper 17 cell generation. Immunity *26*, 371–381.
55. Overacre-Delgoffe, A.E., and Vignali, D.A.A. (2018). Treg Fragility: A Prerequisite for Effective Antitumor Immunity? Cancer Immunol. Res. *6*, 882–887.
56. Tang, Q., Henriksen, K.J., Boden, E.K., Tooley, A.J., Ye, J., Subudhi, S.K., Zheng, X.X., Strom, T.B., and Bluestone, J.A. (2003). Cutting Edge: CD28 controls peripheral homeostasis of CD4^{+}CD25^{+} regulatory T cells. J. Immunol. *171*, 3348–3352.
57. Humrich, J.Y., Cacoub, P., Rosenzwajg, M., Pitoiset, F., Pham, H.P., Guidoux, J., Leroux, D., Vazquez, T., Riemekasten, G., Smolen, J.S., et al. (2022). Low-dose interleukin-2 therapy in active systemic lupus erythematosus (LUPIL-2): a multicentre, double-blind, randomised and placebo-controlled phase II trial. Ann. Rheum. Dis. *81*, 1685–1694.
58. Ward, N.C., Lui, J.B., Hernandez, R., Yu, L., Struthers, M., Xie, J., Santos Savio, A., Dwyer, C.J., Hsiung, S., Yu, A., and Malek, T.R. (2020). Persistent IL-2 receptor signaling by IL-2/CD25 Fusion protein controls diabetes in NOD mice by multiple mechanisms. Diabetes *69*, 2400–2413.
59. Yu, A., Zhu, L., Altman, N.H., and Malek, T.R. (2009). A Low interleukin-2 receptor signaling threshold supports the development and homeostasis of T regulatory cells. Immunity *30*, 204–217.
60. Zheng, G.X.Y., Terry, J.M., Belgrader, P., Ryvkin, P., Bent, Z.W., Wilson, R., Ziraldo, S.B., Wheeler, T.D., McDermott, G.P., Zhu, J., et al. (2017). Massively parallel digital transcriptional profiling of single cells. Nat. Commun. *8*, 14049.
61. Hao, Y., Hao, S., Andersen-Nissen, E., Mauck, W.M., 3rd, Zheng, S., Butler, A., Lee, M.J., Wilk, A.J., Darby, C., Zager, M., et al. (2021).

Integrated analysis of multimodal single-cell data. Cell *184*, 3573–3587.e29.

62. Zappia, L., and Oshlack, A. (2018). Clustering trees: a visualization for evaluating clusterings at multiple resolutions. GigaScience *7*, giy083.
63. Zhang, Y., Park, C., Bennett, C., Thornton, M., and Kim, D. (2021). Rapid and accurate alignment of nucleotide conversion sequencing reads with HISAT-3N. Genome Res. *31*, 1290–1295.
64. Robinson, M.D., McCarthy, D.J., and Smyth, G.K. (2010). edgeR: a Bioconductor package for differential expression analysis of digital gene expression data. Bioinformatics *26*, 139–140.
65. Xu, S., Hu, E., Cai, Y., Xie, Z., Luo, X., Zhan, L., Tang, W., Wang, Q., Liu, B., Wang, R., et al. (2024). Using clusterProfiler to characterize multiomics data. Nat. Protoc. *19*, 3292–3320. https://doi.org/10.1038/s41596-024-01020-z.
66. Wickham, H. (2009). Ggplot2: Elegant Graphics for Data Analysis (Spinger International Publishing Group).

STAR★METHODS

KEY RESOURCES TABLE

REAGENT or RESOURCE	SOURCE	IDENTIFIER
Antibodies		
Alexa Fluor 488 anti-mouse Foxp3	Invitrogen	Cat# 53-5773-82; RRID: AB_763537; Clone FJK-16s
Alexa Fluor 700 anti-mouse CD4	Biolegend	Cat# 116022; RRID: AB_2715958; Clone RM4-5
Alexa Fluor 700 anti-mouse CD8	Invitrogen	Cat# 56-0081-82; RRID: AB_494005; Clone 53–6.7
Alexa Fluor 700 anti-mouse Ki67	BD Pharmingen	Cat# 561277; RRID: AB_10611571; Clone B56
APC anti-mouse CD25	Biolegend	Cat# 102012; RRID: AB_312861; ClonePC61
APC anti-mouse CD4	Biolegend	Cat# 100412; RRID: AB_312697; Clone GK1.5
APC anti-mouse KLRG1	Invitrogen	Cat# 17-5893-81; RRID: AB_469468; Clone 2F1
APC anti-mouse pSTAT5 (Tyr694)	Biolegend	Cat# 936906; RRID: AB_2892500; Clone A17016B.Rec
APC-Cy7 anti-mouse CD44	Biolegend	Cat# 103028; RRID: AB_830785;Clone IM7
APC-Cy7 anti-mouse CD62L	Biolegend	Cat# 104428; RRID: AB_830799; Clone MEL-14
APC-Cy7 anti-mouse CD8	Biolegend	Cat# 100714; RRID: AB_312753; Clone 53–6.7
APC-Cy7 anti-mouse Ly-6C	BD Pharmingen	Cat# 560596; RRID: AB_1727555; Clone AL-21
APC-Cy7 Streptavidin	Biolegend	Cat# 405208
Biotin anti-mouse CXCR5	Biolegend	Cat# 145509; RRID: AB_2562125; Clone L138D7
Brilliant Violet 421 anti-mouse PD1	Biolegend	Cat#135217; RRID: AB_10900085; Clone 29F.1A12
Brilliant Violet 510 anti-mouse CD4	Biolegend	Cat# 100559; RRID: AB_2562608; Clone RM4-5
Brilliant Violet 510 anti-mouse CD45	Biolegend	Cat# 103138; RRID: AB_2563061; Clone 30-F11
Brilliant Violet 605 anti-mouse CD119	BD Pharmingen	Cat# 745111; RRID: AB_2742716; Clone GR20
Brilliant Violet 605 anti-mouse CD25	Biolegend	Cat# 102036; RRID: AB_2563059; Clone PC61
Brilliant Violet 605 anti-mouse CD44	Biolegend	Cat# 103047; RRID: AB_2562451; Clone IM7
Brilliant Violet 768 anti-mouse RORγt	BD Biosciences	Cat# 564723; RRID: AB_2738916; Clone Q31-378
Brilliant Violet 785 anti-mouse CD62L	Biolegend	Cat# 104440; RRID: AB_2629685; Clone MEL-14
eFluor450 anti-mouse IL-17a	Invitrogen	Cat# 48-7177-82; RRID: AB_11149503; Clone eBio17B7
PacBlue anti-mouse CD4	Biolegend	Cat# 100531; RRID: AB_493374; Clone RM4-5
PacBlue anti-mouse CD8	Biolegend	Cat# 100725; RRID: AB_493425; Clone 53–6.7
PE-Cy7 anti-mouse CD127	Biolegend	Cat# 135013; RRID: AB_1937266; Clone A7R34
PE-Cy7 anti-mouse CD25	Biolegend	Cat# 102016; RRID: AB_312865; Clone PC61
PE-Cy7 anti-mouse Interferon-γ	Invitrogen	Cat# 25-7311-82; RRID: AB_469680; Clone XMG1.2
PerCP-Cy5.5 anti-mouse CD8	Biolegend	Cat# 100734; RRID: AB_2075238; Clone 53–6.7
PerCP-Cy5.5 anti-mouse ICOS	Biolegend	Cat# 313518; RRID: AB_10641280; Clone C398.4A
PE/Dazzle 594 anti-mouse CD25	Biolegend	Cat#102048; RRID: AB_2564124; Clone PC61
SuperBright600 anti-mouse CD62L	Invitrogen	Cat# 63-0621-82; RRID: AB_2637416; Clone MEL-14
Chemicals peptides and recombinant proteins		
Bovine serum albumin	Thermofisher	Cat# AM2616
Brefeldin A Solution	Biolegend	Cat# 420601
Collaginase Type III	Worthington	Cat# LS004182
DAPI	Miltenyi	Cat# 130-111-570
DNAse 1	Worthington	Cat# LS002006
EDTA	Thermofisher	Cat# AM9260G
Fetal bovine serum	R&D Systems	Cat# S11150H
Hank's Balances Salt Solution	Thermofisher	Cat# 24020117

(*Continued on next page*)

Continued

REAGENT or RESOURCE	SOURCE	IDENTIFIER
Hank's Balances Salt Solution without Mg^{++} and Ca^{++}	Thermofisher	Cat# 14185052
HEPES	Corning	Cat# 25-060-CI
Ionomycin	Sigma	Cat# I0634
L-glutamine	Thermofisher	Cat# 25030164
2-mercaptoethanol	Thermofisher	Cat #21985023
Monensin Golgi Stop Protein	BD Biosciences	Cat# 51-2092KZ
Penicillin-Streptomycin	Fisher-Scientific	Cat# 15140-122
Percoll	GE	Cat# 17-0891-01
PMA	Sigma	Cat# P1585
RPMI 1640	Corning	Cat #10-040-CV
Sodium azide	Thermofisher	Cat# 190380050
Sodium pyruvate	Thermofisher	Cat# 11360-070
Tamoxifen	Sigma Aldrich	Cat# T5648-1G
ViaStain AOPI Staining Solution	Fisher-Scientific	Cat# NC2019981
Critical commercial assays		
Foxp3 transcription factor staining set	eBioscience	Cat# 00-5523-00
$CD4^+$ T cell Isolation Kit	Miltenyi	Cat# 130-104-454
LS Columns	Miltenyi	Cat# 130-042-401
10X Single Cell 3′ Reagent Kit	10X Genomics	Cat# PN-1000268
Rneasy	Qiagen	Cat# 74104
KAPA RNA Hyperprep with RiboErase (HMR)	Roche	Cat# KK8560
Deposited data		
C57BL/6 genome assembly (mm10)	(Waterson et al., 2002)	http://genome.ucsc.edu/
UCSC Genome Browser	(Kent 2002)	http://genome.ucsc.edu/
scRNAseq (Figures 3 and 4)	This study	NCBI: GSE268024
RNAseq (Figure 2)	This study	NCBI: GSE268024
Experimental models: Organisms/strains		
Mouse: *CD25*$^{FL/FL}$: B6(129S4)-Il2ratm1c(EUCOMM)Wtsi/TrmaJ	(Toomer et al. 2019)[1]	RRID:IMSR_JAX:033093
Mouse: *Foxp3*$^{GFP\text{-}Cre\text{-}ERT2}$: Foxp3tm9(EGFP/cre/ERT2)Ayr/J	(Rubtsov et al. 2010)[31]	RRID:IMSR_JAX:016961
Mouse: *ROSA26*$^{FL\text{-}Stop\text{-}tdTomato}$: B6.Cg-Gt(ROSA)26Sortm9 (CAG-tdTomato)Hze/J	(Madisen et al. 2010)[32]	RRID:IMSR_JAX:007909
Mouse: *IL-2R*^{Y3}	(Yu et al. 2009)[59]	N/A
Oligonucleotides		
All primers	Integrated DNA Technologies	https://www.idtdna.com/
Software and algorithms		
CellRanger version 4.0	(Zheng et al. 2017)[60]	https://www.10xgenomics.com/support/software/cell-ranger/latest
Seurat version 2.3.4 (R Package)	(Hao et al. 2021)[61]	https://satijalab.org/seurat/
Clustree (R Package)	(Zappia and Oshlack 2018)[62]	https://github.com/lazappi/clustree
HISAT2 version 2.2.1	(Zhang et al. 2021)[63]	http://daehwankimlab.github.io/hisat2/

(*Continued on next page*)

Continued

REAGENT or RESOURCE	SOURCE	IDENTIFIER
edgeR (R package)	(Robinson et al. 2010)[64]	https://bioconductor.org/packages/release/bioc/html/edgeR.html
clusterProfiler	(Xu 2024)[65]	https://bioconductor.org/packages/release/bioc/html/clusterProfiler.html
ggplot2 (R package)	(Wickham, 2009)[66]	https://ggplot2.tidyverse.org/
Kaluza	Beckman	https://www.beckman.com/flow-cytometry/software/kaluza
Prism v.10	GraphPad	https://www.graphpad.com/scientific-software/prism/
R	(R Core Team)	https://cran.r-project.org/
Morpheus	Broad Institute	https://software.broadinstitute.org/morpheus/
Other		
Instrument: 10X Chromium Single Cell Controller	10X Genomics	https://www.10xgenomics.com/instruments/chromium-controller
Instrument: Aurora	Cytek	https://cytekbio.com/pages/aurora
Instrument: Bioanalyzer 2100	Agilent	https://www.agilent.com/en/product/automated-electrophoresis/bioanalyzer-systems/bioanalyzer-instrument/2100-bioanalyzer-instrument-228250
Instrument: CytoFLEX LX	Beckman-Coulter	https://www.beckman.com/flow-cytometry/research-flow-cytometers/cytoflex-lx
Instrument: CytoFLEX S	Beckman-Coulter	https://www.beckman.com/flow-cytometry/research-flow-cytometers/cytoflex
Instrument: Nexcelom Cellometer K2	Nexcelom Bioscience	N/A
Instrument: NovaSeq 6000	Illumina	https://www.illumina.com/systems/sequencing-platforms/novaseq.html
Instrument: ProFlex PCR System	Applied Biosystems	https://www.thermofisher.com/us/en/home/life-science/pcr/thermal-cyclers-realtime-instruments/thermal-cyclers/proflex-pcr-system.html?gclid=Cj0KCQjwgrO4BhC2ARIsAKQ7zUngzob6ThGZGZ2jUdy3JaPWwEu8qasTJ65fmF_pxbgZkeNpcTB3a9EaAs6gEALw_wcB&ef_id=Cj0KCQjwgrO4BhC2ARIsAKQ7zUngzob6ThGZGZ2jUdy3JaPWwEu8qasTJ65fmF_pxbgZkeNpcTB3a9EaAs6gEALw_wcB:G:s&s_kwcid=AL!3652!3!683083697661!e!!g!!proflex%20pcr%20system!11227828515!156083344973&cid=bid_mol_pch_r01_co_cp1358_pjt0000_bid00000_0se_gaw_bt_awa_ins&gad_source=1

EXPERIMENTAL MODEL AND STUDY PARTICIPANT DETAILS

Foxp3$^{eGFP\text{-}creERT2}$, R26$^{flox/stop/Tdtomato}$, both on the C57BL/6 genetic background, were purchased from Jackson Laboratory. The CD25$^{fl/fl}$ and IL-2R^{Y3} mutated mice were generated in the lab as previously described.[1,59] All strains were bred within the specific pathogen-free animal facility at the University of Miami. Genotyping of strains was performed by PCR amplification using the primers and protocols recommended by Jackson Laboratory. Females and males were included in all studies except only female mice were used for RNAseq and scRNAseq studies. The influence of sex was not studied and may represent a limitation to the research's generalizability. Mice were typically used when they were 8-12 weeks of age. Mice were not specifically randomly assigned to experimental groups. Animal studies were reviewed and approved by the Institutional Animal Care and Use Committee at the University of Miami (Protocol 22-128).

CD25$^{fl/fl}$Foxp3$^{eGFP\text{-}CreERT2}$R26^{tomato} (CD25^{iKO}) mice and CD25$^{wt/wt}$Foxp3$^{eGFP\text{-}CreERT2}$R26^{tomato} (CD25^{WT}) mice were treated with tamoxifen by intraperitoneal injection. Tamoxifen was dissolved in corn oil at 20 mg/mL and 100 μl were injected daily for 5 consecutive days. Mice were sacrificed 10 days after completion of tamoxifen unless otherwise specified.

METHOD DETAILS

Lymphocyte isolation

Single-cell suspensions from the spleen and lymph nodes were obtained by mechanical disruption in cold 1X Hank's balanced salt solution (HBSS). Red blood cells were lysed by incubating cells in ammonium-chloride-potassium buffer in 37° C water bath for 1 minute. Cells were washed with HBSS and filtered using a 70 μm mesh prior to cell surface staining.

Small intestinal lymphocytes were harvested by dissecting the small intestine 0.5cm distal to the stomach and 0.5cm proximal to the cecum. The flat end of forceps was used to push out fecal matter and the lumen was distended with a probe to reveal the Peyer's patches. After the Peyer's patches were removed using forceps and fine-tipped scissors, the lumen of the small intestine was revealed with scissors, and mucus was removed by gently scraping with the flat end of forceps. The remaining intestinal tissue was transferred to a petri dish and minced very finely with scissors in 5mL wash buffer (calcium- and magnesium-free HBSS containing 2.5% fetal bovine serum, 100U/mL penicillin, 100ug/mL streptomycin and 2mM L-glutamine). The contents of the petri dish were transferred to a 50mL tube and washed twice in 25mL wash buffer. The intestinal epithelium of these pieces was removed by incubating for 15 minutes at 37° C with gentle agitation in 30mL calcium- and magnesium-free HBSS containing 10% fetal bovine serum, 5mM EDTA and 15mM HEPES (EDTA buffer). After incubation, the tissue pieces were allowed to settle by gravity and the supernatant was poured off to discard the intraepithelial lymphocytes. The tissue was resuspended in another 30mL of EDTA buffer and incubated for another 15 minutes with gentle agitation. The tissue was again allowed to settle by gravity and the supernatant was poured off and discarded. Next, the tissues was washed twice in 25mL of wash buffer. After decanting, the tissue was resuspended in 30mL wash buffer with 300 U/mL Collagenase Type 3 (Worthington Cat# LS004182) and 10 μg/mL DNAse I (Worthington Cat# LS002006). After allowing the large pieces of tissue to settle to the bottom of the tube, they were taken up in 5-10 ml of buffer using a 10mL stripette, transferred to a petri dish and minced with fine-tipped scissors. The contents of the petri dish were then added back to the remaining sample in the 50mL digestion tube and incubated for 40 min at 37° C with gentle agitation. After allowing the large pieces of tissue to settle to the bottom of the tube, the tissue was again transferred to a petri dish in the same manner and pipetted against the dish 10 times to further break up the pieces. The contents of the petri dish were added back to the remaining sample in the 50mL digestion tube and allowed to digest for another 15 minutes at 37°C with gentle agitation. Cells were washed in wash buffer and filtered. Lymphocytes were isolated using a 40/70% Percoll gradient (GE 1.130g/mL Cat#17-0891-01) and centrifuged at 700g for 20 min at room temperature with no brake. Lymphocytes preps were then used for downstream analyses.

Flow cytometry and FACS

All labeled antibodies with their sources and working concentrations used for flow cytometry and FACS are reported in the key resources table. Cells were incubated in anti-CD16/CD32 (2.4G2) prior to cell surface staining and washed in staining buffer (HBSS containing 0.2% BSA and 0.1% (w/v) sodium azide). Extracellular staining was performed on 3.0 x 10^6 cells in staining buffer for 20 min at 4°C in the dark.

Fixation for intracellular staining was performed using the eBioscience Foxp3/transcription factor staining buffer set (Cat#00-5523-00). 3.0 x 10^6 cells were resuspended in 500 μl of diluted fixation buffer for 30 minutes at 4° C in the dark. Cells were then washed in permeabilization buffer and intracellular staining was performed in permeabilization buffer at 4°C in the dark for 30 minutes.

For flow cytometric analyses, cells were washed, filtered a second time, and run a CytoFLEX (Beckman Coulter) or Aurora Cytek (BD Biosciences) and analyzed using Kaluza software.

For cell sorting, $CD4^+$ T cells were isolated by negative selection using the $CD4^+$ T Cell Isolation Kit (Miltenyi #130-104-454 and LS Columns, Miltenyi #130-042-401). Cells were resuspended in sorting buffer; DAPI (Miltenyi #130-111-570) was used at a final concentration of 0.1 μg/mL for viability; and sorting was performed using a BD FACS Aria-II system. Cells were sorted into RPMI-1640 media supplemented with 10% fetal bovine serum (FBS).

Adoptive transfer

$CD25^{WT}$ and $CD25^{iKO}$ female animals were induced with tamoxifen and sacrificed 5 days after completion of tamoxifen. Spleens and lymph nodes were prepped for sorting as described above. $GFP^+tomato^+CD62L^{hi}$ and $GFP^+tomato^+CD62L^{lo}$ Treg subsets were isolated from both groups. Isolated cells were washed twice in cold PBS. 3x10^5 cells in 100ul PBS were injected into the tail vein of $IL2R^{Y3}$ recipient mice. Recipient mice were sacrificed 7 days after transfers and spleens were prepared for flow as described above. Due to the low abundance of transferred cells, 10^7 splenocytes were analyzed per sample.

Single Cell RNA-seq

Splenocytes from $CD25^{WT}$ and $CD25^{iKO}$ female mice (pooled from n=2-3 per group) were prepared and sorted as described above. GFP^+ $tomato^+$ Tregs were isolated from each group. Cells were sorted into 0.04%BSA in PBS and submitted to the University of Miami Oncogenomics Core for library preparation and sequencing at a final concentration of 1000 cells/μl. Viability for all sequencing samples was >93% as measured by Nexcelom Cellometer K2 with ViaStain AOPI Staining Solution. Washed cells were then encapsulated in a 10× Chromium Single Cell Controller, and libraries were constructed using the 10× Single Cell 3′ Reagent Kit. Completed libraries were sequenced on the NovaSeq 6000 platform at a target of 50,000 reads per cell per sample. Reads were aligned to the mm10 genome using CellRanger (version 4.0).[60] Seurat (version 2.3.4)[61] was used to apply cutoffs for read quality, doublets and high mitochondrial RNA sequences (low viability). Only cells that met the following cutoffs were included in the analysis: feature number 500-3000, total read count <12000, percent mitochondrial

reads < 7.5%. Principle component analysis was performed, and the top components were included based on Jackstraw plots in the UMAP analysis at a range of resolutions. Clustree (R package)[62] was used to visualize the division of clusters with increasing resolution (0.1-1.0).

RNA-seq

At least 1x10^6 FACS-purified $CD25^{iKO}$ Treg subsets and their WT counterparts were pelleted and resuspended in 350ul of Buffer RLT (RNeasy, Qiagen #74104). Cells were homogenized by vortexing for 1 minute. At this point, samples were stored in Buffer RLT at -80°C for up to two weeks prior to RNA isolation. RNA was prepared using the RNeasy kit following Qiagen's protocol for isolation of total RNA from animal cells using spin technology. The Oncogenomics Core at the University of Miami conducted quality control, library preparation and sequencing. Quality control was performed on the Bioanalyzer 2100 (Agilent). Libraries were prepared using KAPA's RNA Hyperprep protocol with RiboErase (HMR) kit for rRNA depletion and sequencing was performed on 100bp pair-end reads using the Illumina NovaSeq 6000 using a S1-200 reagent kit.

RNAseq reads were mapped to the *Mus musculus* genome mm10 using HISAT2 (ver.2.2.1) aligner.[63] Raw counts were generated using the mm10 reference based on UCSC annotations. Differentially expressed genes (DEGs) between experimental groups were identified using edgeR[64] with a log fold-change cutoff of 0.5 and adjusted p-value < 0.05. DEG testing was performed using glmQLF between the following four comparisons: $CD25^{iKO}$ vs $CD25^{WT}$ cTregs, $CD25^{iKO}$ vs $CD25^{WT}$ eTregs, $CD25^{iKO}$ cTregs vs $CD25^{iKO}$ eTregs and $CD25^{WT}$ cTregs vs $CD25^{WT}$ eTregs. Positive and negative DEG lists were analyzed using clusterProfiler[65] to determine upregulated and downregulated pathways using multiple databases. Transcripts per million (TPM) were used to generate heat maps using Morpheus (Broad Institute; https://software.broadinstitute.org/morpheus/) by converting to *Z* score and performing hierarchical clustering. Sequencing data was displayed using ggplot2.[66]

Cytokine staining

$CD25^{WT}$ and $CD25^{iKO}$ mice were induced with tamoxifen and euthanized 26 days after completion of tamoxifen. Lymphocytes from the mesenteric lymph nodes and the lamina propria were isolated as described above. 500,000 cells cultured in a 96-well flat-bottom tissue culture plate in 300 μl RPMI-1640 media supplemented with 5% fetal bovine serum (FBS), 100 U/mL penicillin, 100 μg/ mL streptomycin, 2 mM L-glutamine, 0.05 mM β-mercaptoethanol, and 1 mM sodium pyruvate (RPMI-CM). The cells were stimulated with PMA (50 ng/ml; Sigma P1585) and ionomycin (1 μM; Sigma, Cat I0634), as indicated. Stock solutions for PMA (100 μg/ml) and ionomycin (1 mM) were dissolved in 100% ethanol or DMSO, respectively, and these were then diluted in RPMI-CM. All cultures also contained monensin (1:1000, BD GolgiStop Protein Transport Inhibitor, BD Biosciences, Cat. No. 51-2092KZ), and 5 μg/mL Brefeldin A (BioLegend Brefeldin A Solution, Cat. No. 420601). Cells were then cultured for 4 hours at 37°C in 5% CO2. Cells were harvested and prepared for flow cytometric analysis as described above.

QUANTIFICATION AND STATISTICAL ANALYSIS

Data was analyzed and plotted using Graphpad Prism V.10. Individual dot plots include the mean +/- SD. Unpaired t-tests were used to analyze the significance between groups. When determining if there is a significance between two qualitative variables, a Fisher's exact test was used. Significance is indicated by * = p<0.05, ** = p<0.01, *** = p<0.001, and **** = p<0.0001. The statistical details of the experiments are found in the figure legends.